

## Isotope Geochemistry (O, C, S, Sr) and Rb–Sr Age of Carbonatites in Central Tuva

A. V. Nikiforov<sup>a\*</sup>, A. V. Bolonin<sup>a</sup>, B. G. Pokrovsky<sup>b</sup>, A. M. Sugorakova<sup>c</sup>,  
A. V. Chugaev<sup>a</sup>, and D. A. Lykhin<sup>a</sup>

<sup>a</sup> *Institute of Geology of Ore Deposits, Petrography, Mineralogy, and Geochemistry, Russian Academy of Sciences, Staromonetnyi per. 35, Moscow, 119017 Russia*

<sup>b</sup> *Geological Institute, Russian Academy of Sciences, Pyzhevskii per. 7, Moscow, 119017 Russia*

<sup>c</sup> *Tuvian Institute of Comprehensive Development of Natural Resources, Siberian Division, Russian Academy of Sciences, ul. Internatsional'naya 117a, Kyzyl, 667007 Republic of Tyva, Russia*

Received January 16, 2006

**Abstract**—The Rb–Sr isochron age of igneous ankerite–calcite and siderite carbonatites in central Tuva is estimated at  $118 \pm 9$  Ma. The following ranges of initial values of O, C, Sr, and sulfide and sulfate S isotopic compositions were established:  $\delta^{18}\text{O}_{\text{carb}} = +(8.8\text{--}14.7)\%$ ,  $\delta^{13}\text{C}_{\text{carb}} = -(3.6\text{--}4.9)\%$ ,  $\delta^{18}\text{O}_{\text{quartz}} = +(11.6\text{--}13.7)\%$ ,  $\delta^{34}\text{S}_{\text{pyrite}} = +(0.3\text{--}1.1)\%$ , and  $(^{87}\text{Sr}/^{86}\text{Sr})_i = 0.7042\text{--}0.7048$  for ankerite–calcite carbonatite and  $\delta^{18}\text{O}_{\text{sid}} = +(9.2\text{--}12.4)\%$ ,  $\delta^{13}\text{C}_{\text{sid}} = -(3.9\text{--}5.9)\%$ ,  $\delta^{18}\text{O}_{\text{quartz}} = +(11.2\text{--}11.4)\%$ ,  $\delta^{34}\text{S}_{\text{pyrite}} = -(4.4\text{--}1.8)\%$ ,  $\delta^{34}\text{S}_{\text{sulfate}} = +(8.6\text{--}14.5)\%$ , and  $(^{87}\text{Sr}/^{86}\text{Sr})_i = 0.7042\text{--}0.7045$  for siderite carbonatite. The obtained isotopic characteristics indicate that both varieties of carbonatites are cognate and their mantle source is comparable with the sources of Late Mesozoic carbonatites in the western Transbaikalian region and Mongolia. The revealed heterogeneity of isotopic compositions of carbonatites is caused by their contamination with country rocks, replacement with hydrothermal celestine, and supergene alteration.

**DOI:** 10.1134/S1075701506040027

### INTRODUCTION

New data on the Late Mesozoic carbonatitic magmatism in Central Asia have been obtained in recent years. The carbonatite occurrences of this age, which were found in the western Transbaikalian region (the Khalyuta and Arshan complexes) and in the South Hangay in Mongolia (Mushgia Complex, etc.), are distinguished by high Sr, Ba, LREE, P, S, and F concentrations along with low Nb and Ta contents. The REE fluorite–barite–siderite ore and associated ankerite–calcite rocks of the Karasug deposit in Tuva are close to these carbonatites in bulk composition and geochemical signature. Some authors classified these rocks as carbonatites (Puzanov, 1975; Bolonin et al., 1984), and others, as products of hydrothermal activity (Ontoev, 1963; Khomyakov and Semenov, 1971; Kulik and Mel'gunov, 1992). Their age also remained uncertain. Recently, we performed isotopic and geochemical investigations of the Karasug deposit and several other occurrences in central Tuva that were not covered in the literature. The results of geological studies concerning the dimensions, abundance, localization, and internal structure of carbonatite bodies, as well as their modal and chemical compositions, were discussed by Nikiforov et al. (2005). These data confirmed that the stud-

ied rocks belong to carbonatites. In this paper, we present the results of isotopic studies that allowed us to estimate the age of carbonate rocks and to demonstrate their compositional and genetic similarity to carbonatites known from other provinces.

### GEOLOGY OF CARBONATITES

Several occurrences of carbonatites similar in composition, structure, and formation conditions are known in central Tuva. They are hosted in Paleozoic volcanic and terrigenous rocks and related to large latitudinal fault zones, which also control small granitoid and basic intrusions. The carbonatite occurrences are clustered in spatially separate fields that are traceable as a near-meridional belt extending across the strike of the main Paleozoic structural features (Fig. 1). The largest (Karasug) carbonatite field (ore field, or deposit) is located in the Ordovician and Silurian rocks at the wall of the Devonian Tuva Trough. The Chailyukhem ore occurrence is situated in the Kurtushibinsky Range 68 km north of the Karasug field. Carbonatites of the Chaakhol field crop out southerly, within the Devonian trough, on the northern slope of the West Tannu-Ola Range. Carbonatites of the Choza–Ulatai district, including the Ulatai, Teeli–Orgudyd, and North and South Choza fields, are located on the southern slope of this range. Carbonatites occur as large pipelike bodies

\*Address for correspondence: A.V. Nikiforov. E-mail: nikav@igem.ru

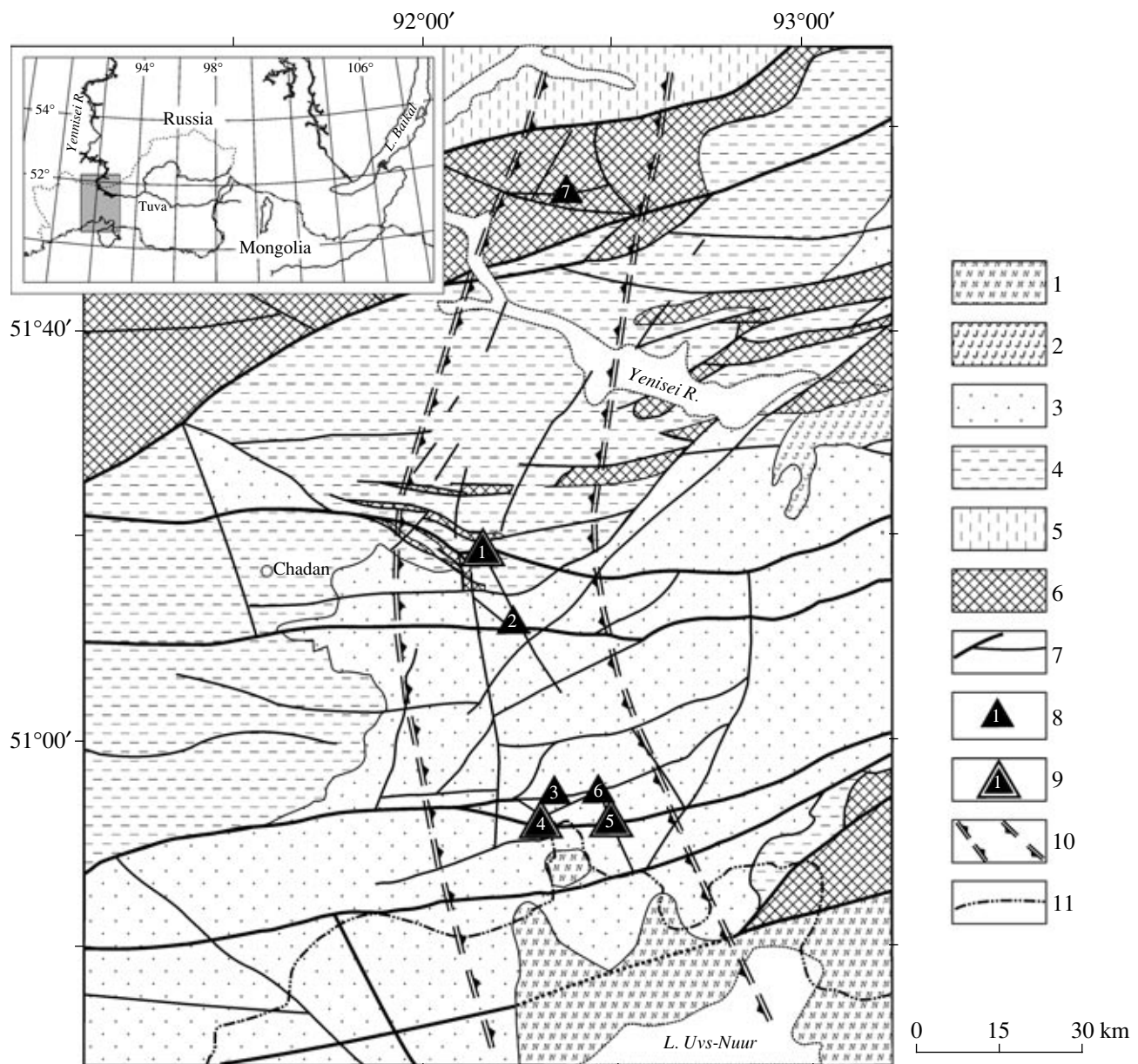


**Fig. 1.** Geologic map of the area of carbonatite occurrences in central Tuva, compiled after *Geological Map ...* (1983). (1) Neogene and Quaternary loose sediments; (2) Jurassic gray sandstone, siltstone, mudstone, and coal; (3) Tuva Trough: Devonian–Carboniferous sandstone, siltstone, gravelstone, limestone, marlstone, tuffite, and basic and silicic volcanics at the base of the section; (4) Khemchik–Sistigkhem Trough: Ordovician–Silurian sandstone, siltstone, gravelstone, and limestone; (5) West Sayan Block: Ordovician–Silurian sandstone, mudstone, and limestone; (6) Neoproterozoic–Lower Cambrian schist, quartzite, metabasic rocks, and limestone; (7) faults; (8) carbonatite fields: Karasug (1), Chaakhol (2), Teeli–Orgudyd (3), Ulatai (4), South Choza (5), North Choza (6), Chailyukhem (7); (9) carbonatite fields sampled for Rb–Sr dating; (10) near-meridional belt of carbonatite fields; (11) state border of the Russian Federation.

up to 700 m in diameter, steeply dipping dikelike bodies 100–160 m thick, and thin veins. Contacts of carbonatites with country rocks are mostly sharp and crosscutting. In some places, carbonatites occur as a cement of breccia or veinlet stockworks.

Carbonatites are represented by ankerite–calcite (the first intrusive phase) and ore-bearing siderite (the second phase) varieties. The latter is a multicomponent ore (REE, Sr, Ba, Fe, and fluorite).

Ankerite–calcite carbonatite is a white, fine-to-medium-grained (0.5–5 mm) massive rock. Rhombohedral ankerite crystals are incorporated into an aggregate of equant calcite grains; euhedral grains of pyrite, apatite, quartz, and muscovite are second in abundance; monazite and parisite are accessory minerals (Fig. 2).

Siderite carbonatite is a fine-to-medium-grained rock with massive and occasionally oriented texture and porphyritic structure. Phenocrysts of white barite

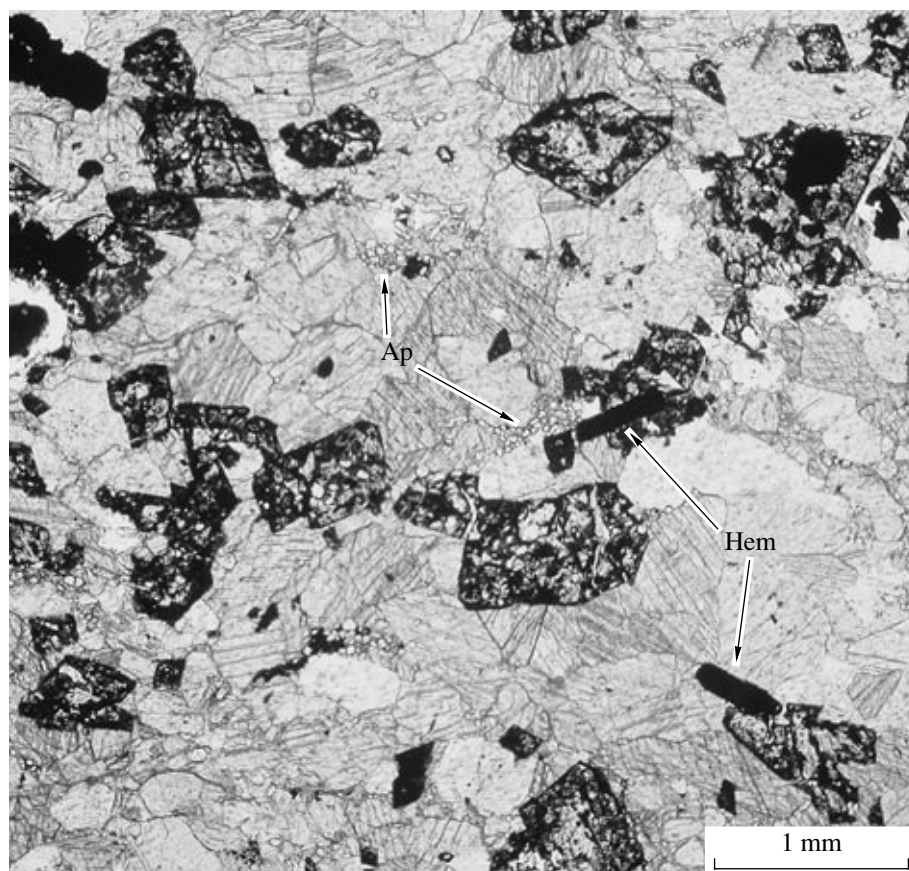


**Fig. 2.** Ankerite–calcite carbonatite. Photomicrograph Uch-5/1, plane light. Dark rhombohedrons are oxidized ankerite crystals in calcite matrix; (Ap) apatite, (Hem) hematite.

and violet fluorite, as well as pyrite, quartz, muscovite, bastnaesite, apatite, and accessory monazite, uraninite, and molybdenite, are uniformly distributed through the light gray aggregate of siderite grains (Fig. 3). Siderite occurs as both rhombohedral phenocrysts and a fine-grained groundmass that also contains fluorite. It is significant that the habit and dimensions of phenocrysts of low-abundance minerals are similar in carbonatites of both types. Quartz (Figs. 4a, 4b) and apatite are dipyramidal hexagonal prismatic crystals; pyrite is observed as faceted grains of complex morphology; muscovite, as hexagonal sheets; and bastnaesite and parisite, as tabular crystals.

Carbonatites always contain small angular fragments of the country aluminosilicate rocks partly greisenized up to the formation of quartz–muscovite greisen. Greisen-like fine-grained quartz–muscovite aggregates are formed as products of partial assimilation of country rock fragments by carbonatites. Muscovite crystals occasionally occur at contacts of such fragments with carbonatite. In addition to muscovite, which is closely related to fragments of country rocks and occurs within these fragments or at their periphery, pale greenish transparent packets of hexagonal tabular Fe-rich muscovite crystals, in some cases more than a mil-

limeter in size, are uniformly dispersed throughout carbonatite (Figs. 5a, 5b). Muscovite is intergrown with rock-forming carbonates showing no signs of reaction between them. The muscovite content is commonly insignificant (from single grains to 2 vol %); some samples demonstrate a positive correlation between the amounts of dispersed mica and fragments of country rocks. Relics of aluminosilicate rocks might have served as centers of mica crystallization and as the main source of Al, K, and Si for muscovite formation. Most likely, muscovite crystallized in equilibrium with rock-forming carbonates, as supported by a high FeO content (6.3 wt %) in muscovite dispersed throughout siderite carbonatite. In its optical properties ( $N_g = 1.607$ ,  $N_m = 1.604$ ,  $2V = 15^\circ\text{--}20^\circ$ ), the Fe-rich muscovite from carbonatites differs from muscovite that is contained in fragments of greisenized granite ( $N_g = 1.606$ ,  $N_p = 1.566$ ,  $2V = 39^\circ\text{--}40^\circ$ ) (Bolonin and Nikiforov, 2004).

A two-phase injection mechanism of carbonatite formation under conditions of subvolcanic depth facies (Bolonin, 1999; Nikiforov et al., 2005) is supported by the morphology of carbonatite bodies, their structural and textural attributes (see above), the occurrence of angular fragments of country rocks, insignificant replacements of these fragments with carbonates, and

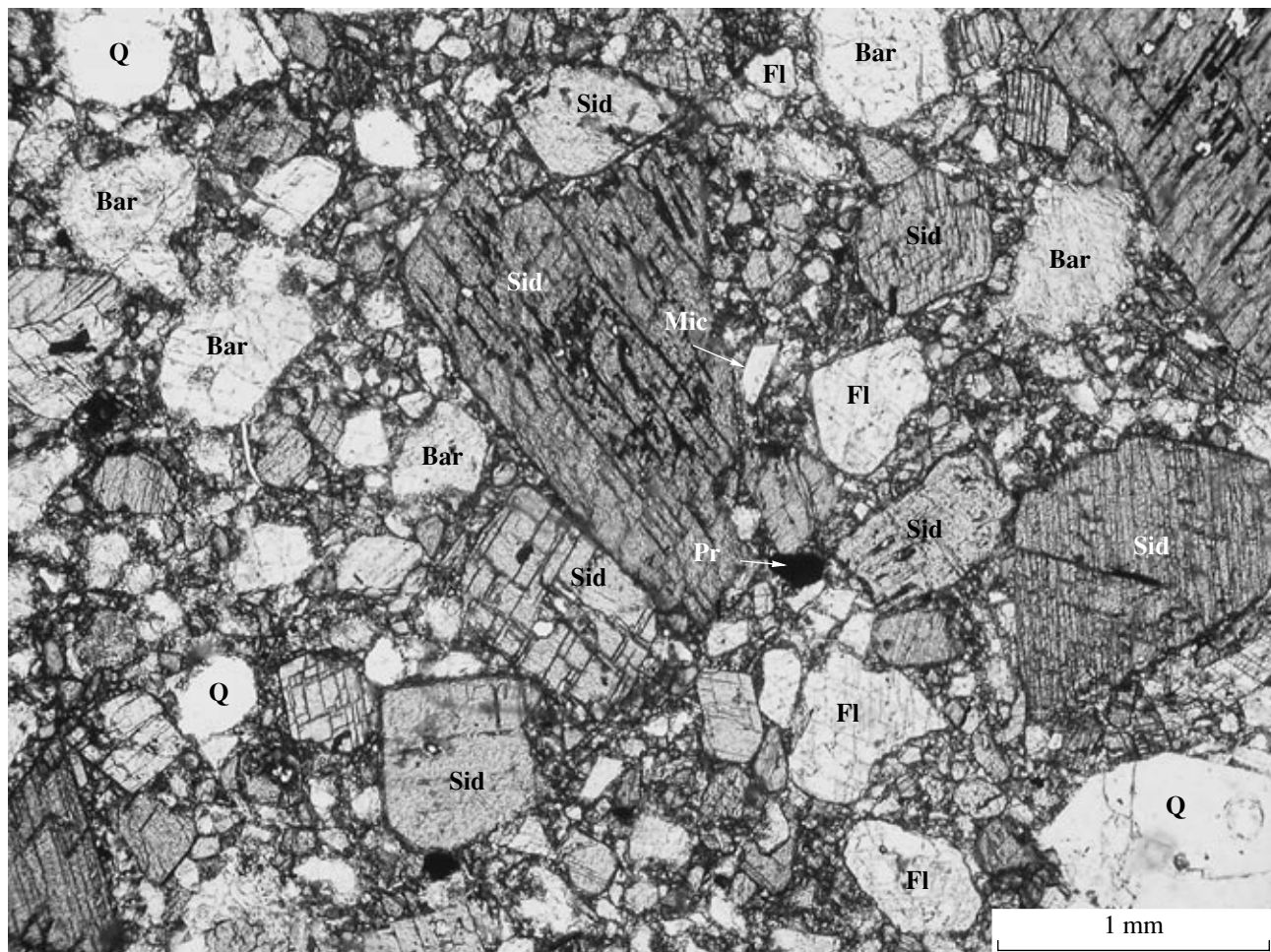


**Fig. 3.** Siderite carbonatite. Photomicrograph Ks-4/1, plane light. (Sid) siderite, (Bar) baritocelastine, (Fl) fluorite, (Q) quartz, (Mic) Fe-rich muscovite, (Pr) pyrite.

automagmatic crushing of carbonatites and their phenocrysts. The homogenization temperature of brine–melt inclusions in fluorite reaches 650–750°C (Kandinov and Kharlamov, 1978).

After injection, the greater part of siderite carbonatites were affected by autometamorphic alteration, first by high-temperature replacement with hematite that also involved ankerite–calcite carbonatite and afterwards by hydrothermal replacement with celestine. Hematite disseminations as small tabular crystals of specularite are dispersed in the carbonate matrix (Fig. 6). Such crystals vary from 0.1 to 10 mm in size, and the amount of hematite in rocks ranges from single grains to 70 vol %. Crystallization of hematite is not accompanied by recrystallization of carbonates. Baritocelastine and celestine pseudomorphs after barite phenocrysts and replacements of fine-grained fluorite–siderite aggregates with celestine were established only in particular carbonatite bodies of the Karasug field. Siderite carbonatites with baritocelastine were described by Bolonin and Nikiforov (2004). The temperature range of celestine formation probably equals 140–

250°C; this is the homogenization temperature of fluid inclusions in the late fluorite veinlets associated with baritocelastine (Kandinov and Kharlamov, 1978).

The supergene alteration of carbonatites in all fields of central Tuva is related to the weathering that developed in the Paleogene. The depth of the oxidation zone reaches 300 m in the Karasug field and is variable elsewhere, not exceeding 100 m. Under supergene conditions, siderite, ankerite, and pyrite were replaced almost completely with goethite, hydrogoethite, hydrohematite, and limonite. Porous, dark brown hematite–goethite–hydrogoethite or yellow-brown limonite rocks with remaining unaltered fluorite and barite crystals are the final products of oxidation of siderite carbonatite. The initially white ankerite–calcite carbonatite, being oxidized, is transformed into a spotty rock colored with brown iron hydroxides. Ankerite begins to oxidize first. Hydrogoethite and calcite aggregates (<1–2 vol %) appear along grain boundaries and cleavage planes; eventually, full pseudomorphs of hydrogoethite and fine-grained calcite replace ankerite (Fig. 7a). White primary calcite is also altered. As can be seen

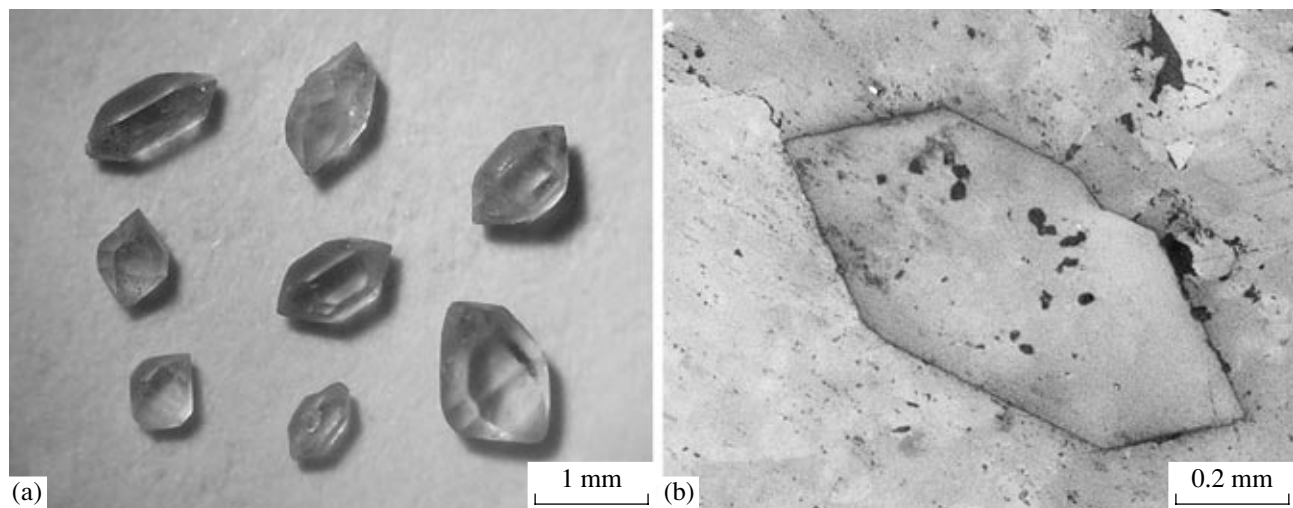


**Fig. 4.** Quartz crystals from (a) ankerite–calcite and (b) siderite carbonatites. (a) Grains picked out under a binocular microscope; (b) polished section Chkh-4.

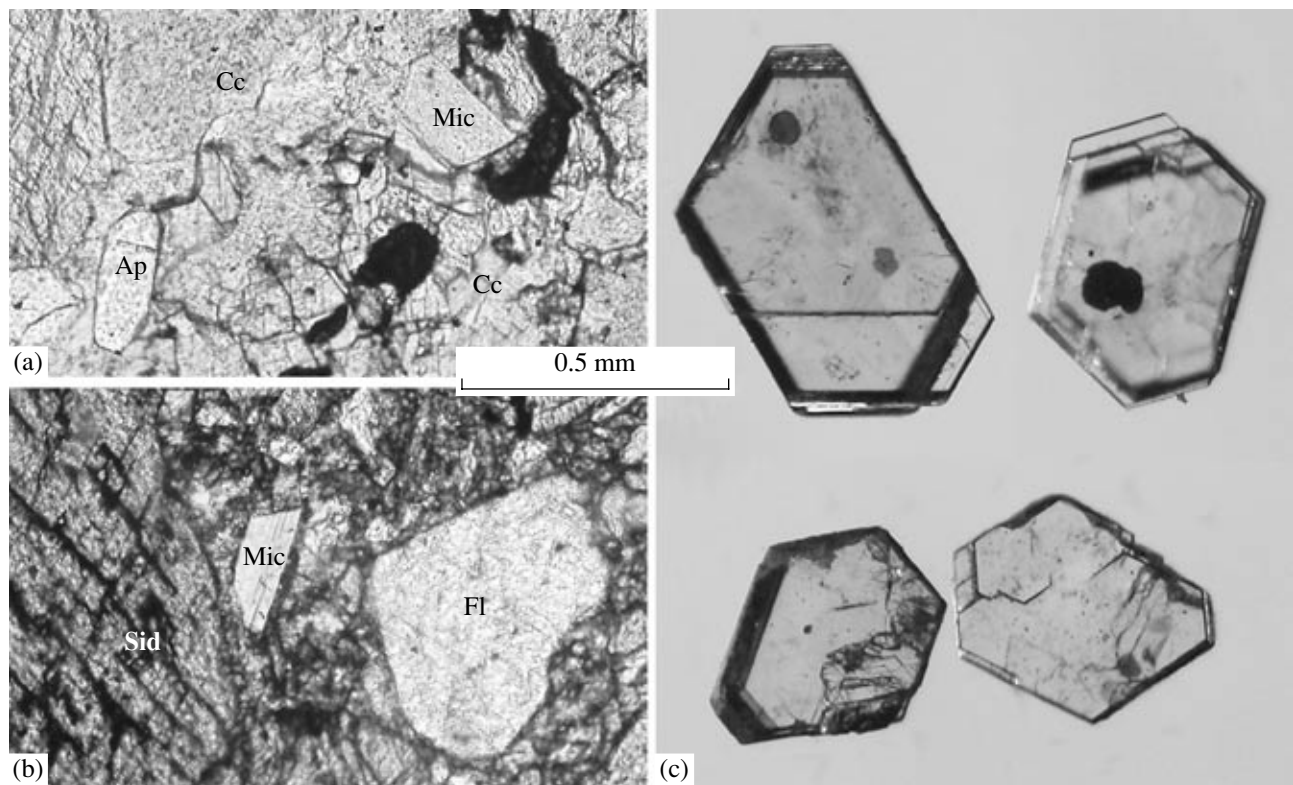


**Fig. 5.** Mica crystals in carbonatite matrix. (a) Ankerite–calcite carbonatite, photomicrograph Uch-19/3, plane light; (b) siderite carbonatite, photomicrograph Ks-4/1, plane light; (c) mica crystals picked out under a binocular microscope for isotopic Rb–Sr analysis. (Mic) Fe-rich muscovite, (Sid) siderite, (Fl) fluorite, (Ap) apatite, (Cc) calcite; dark is iron hydroxides.

under a microscope, it becomes turbid and acquires a brownish hue due to the fine disseminations of iron hydroxides (Fig. 7b). Calcite grains are often recrystallized and freed from impurities along separate microfractures. In the inner parts of recrystallized zones, a

coarse-grained aggregate of the transparent newly formed calcite grades into geodes and extended veinlets.

Strontianite occurs in the oxidation zone and the upper parts of unoxidized carbonatites at the Karasug



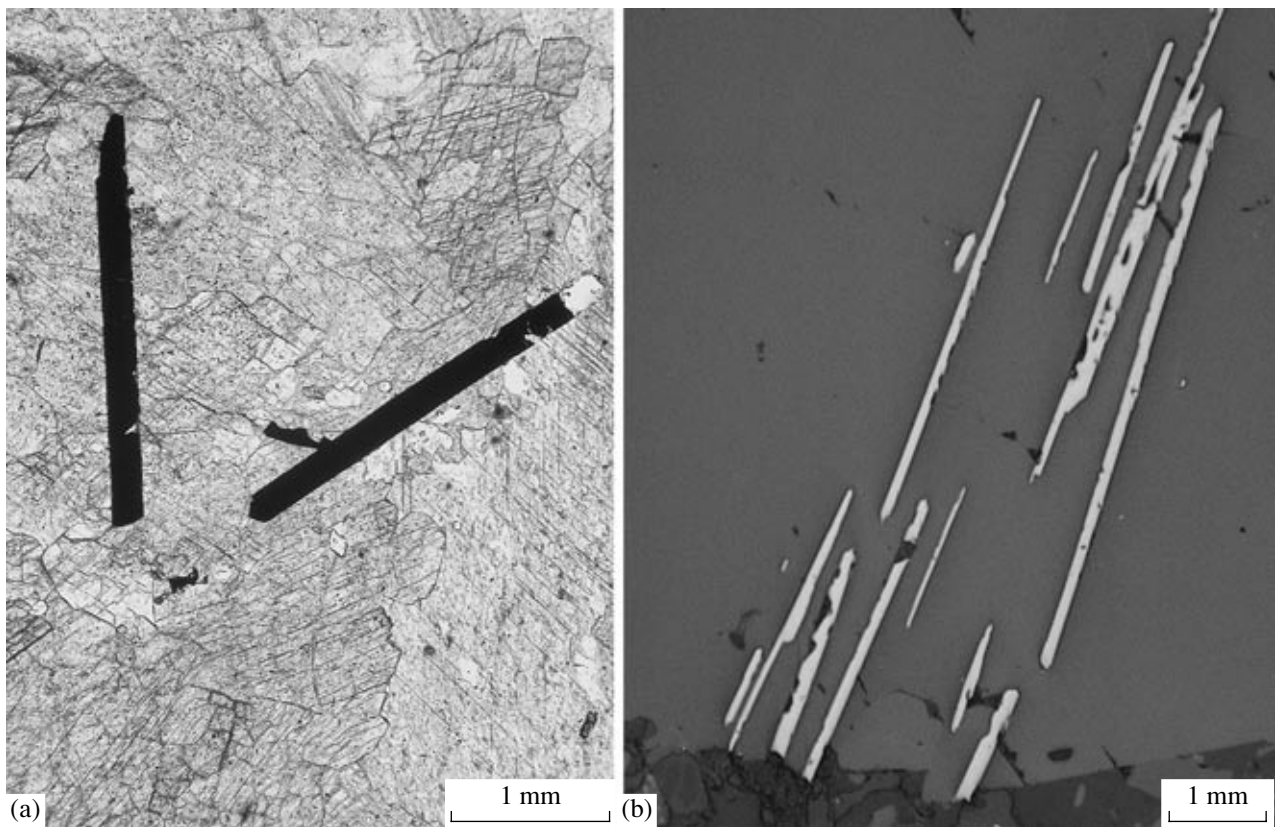


**Fig. 6.** Hematite metacrysts in (a) ankerite–calcite carbonatite, photomicrograph Uch-18, and (b) in siderite phenocryst, polished section Ks-6/68.

deposit as metasomatic aggregates and veinlets. Some authors refer the strontianite mineralization to products of the final stage of hydrothermal activity (Ontoev, 1963). However, available evidence indicates its supergene nature (Bolonin et al., 1984).

Quartz–carbonate veins as thick as 20 cm with inequigranular coarse-grained texture and symmetric zoning and distinguished by the absence of rare-metal mineralization (barren hydrothermal veins) are observed in the Karasug, Chaakhol, and Teeli–Orgudyd fields. Fragments of such veins are occasionally found in carbonatites. Their genetic relations to carbonatites remain ambiguous. For comparative purposes, we determined the O and C isotopic composition in carbonates from these veins.

The age of carbonatites in central Tuva cannot be established on the basis of geological data. The youngest country rocks in the Chaakhol, North Choza, and Teeli–Orgudyd fields are Upper Devonian. As follows from indirect evidence, carbonatites were formed in the post-Carboniferous time because the belt of carbonatite fields crosses the trough filled with Devonian–Carboniferous sedimentary rocks (Fig. 1). The upper age boundary of carbonatites is determined by the fact that they were weathered and oxidized in the Palogene. Fragments of oxidized siderite carbonatites from the

Karasug deposit were found in valley fill that contains a spore–pollen complex of Oligocene age (Shorygina, 1960).

The age of rocks from the Karasug deposit was determined in the 1960s with the K–Ar and U–Pb methods (Shurupov et al., 1966). The minerals used for the dating were not directly related to carbonatites. The following results were obtained: biotite from a xenolith of feldspathized and hydrothermally altered plagiogranite yielded 151 Ma; biotite from metasomatic glimmerite, 132 Ma; muscovite from quartz–muscovite greisen, 124 Ma; hydrothermally altered granitoids, 122 and 114 Ma; and microcline from quartz–carbonate rocks near the contact of orebodies, 66 Ma. Most of the above dates are related to remnants of older granitoid rocks and their xenoliths incorporated into carbonatites. These rocks underwent diverse alterations, whose sequence, as well as their relationships with certain geologic events, in particular, with carbonatite formation, has remained a matter of debate (Nikiforov et al., 2005); the scattered age estimates confirm these uncertainties. Carbonatites proper were dated with the Th–U–Pb method; however, the results published by Shurupov et al. (1966) turned out to be equivocal. Uraninite from siderite ore yielded 75 Ma ( $^{206}\text{Pb}/^{238}\text{U}$ ), and bastnaesite from hematite veins was dated at 69 Ma

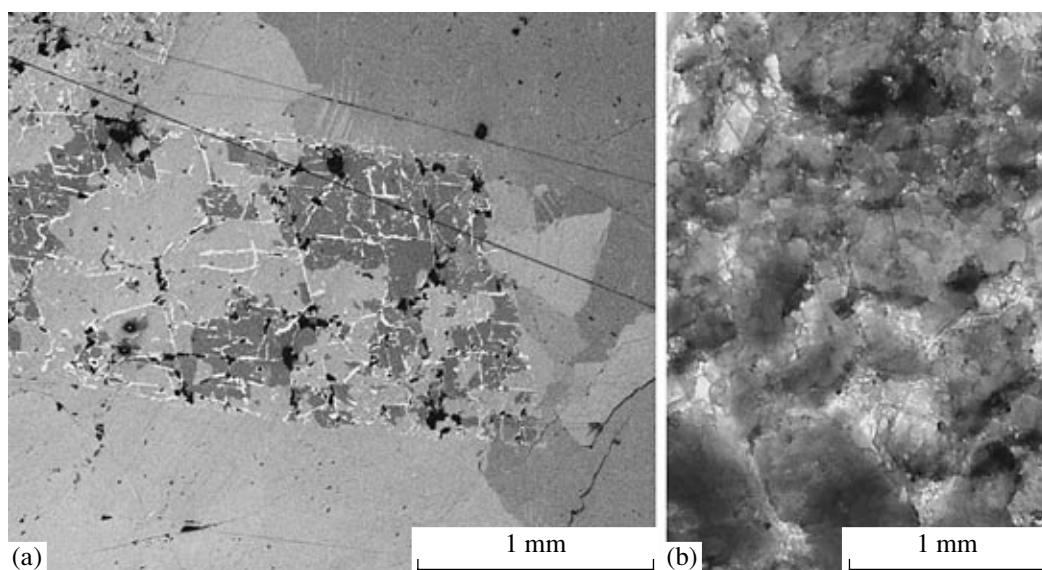


**Fig. 7.** Oxidation of ankerite–calcite carbonatite. (a) Pseudomorphs of iron hydroxides (white) and calcite after rhombohedral ankerite crystal, photomicrograph Uch-77, crossed polars; (b) recrystallization of primary calcite, polished plate Uch-48. Calcite colored by iron hydroxides is gray and turbid; areas of newly formed calcite are light.

( $^{206}\text{Pb}/^{238}\text{U}$ ), 33 Ma ( $^{207}\text{Pb}/^{235}\text{U}$ ), and 72 Ma ( $^{208}\text{Pb}/^{232}\text{Th}$ ). These discordant values indicate that the isotopic system was disturbed, and the results obtained are hardly correct.

#### RESEARCH METHODS

The Rb–Sr studies were carried out at the Laboratory of Isotope Geology and Geochronology of the Institute of Geology of Ore Deposits, Petrography, Mineralogy, and Geochemistry, Russian Academy of Sciences (RAS), using the standard technique (Chernyshev et al., 1983; Zhuravlev et al., 1983) and the isotope dilution method. The Rb–Sr spike enriched in  $^{85}\text{Rb}$ ,  $^{84}\text{Sr}$ , and  $^{88}\text{Sr}$  was used. The total level of background contamination of a sample during its chemical preparation and subsequent isotopic analysis was below 0.05 ng Rb and 0.15 ng Sr. The isotope ratios of Rb and Sr were measured on a Sector-54 mass spectrometer in the static and multidynamic regimes, respectively. The uncertainty of  $^{87}\text{Rb}/^{86}\text{Sr}$  ratio was not higher than 1% ( $\pm 2\sigma$ ). The accuracy of measurements of the  $^{87}\text{Sr}/^{86}\text{Sr}$  ratio was controlled by the results of analysis of an SRM-987 standard sample. The reproducibility of SRM-987 over the period of measurements was  $^{87}\text{Sr}/^{86}\text{Sr} = 0.710245 \pm 24$  ( $\pm 2\sigma$ , 16 measurements). The isochron parameters were calculated with the ISOPLOT/Ex. Version 2.06 program (Ludwig, 2001).

Carbon, oxygen, and sulfur isotopic compositions were determined at the Laboratory of Isotope Geochemistry and Geochronology of the Geological Institute, RAS. Charges of mineral monofractions 50–100 mg in weight were used for the analysis. After

crushing of hand specimens and sieving, the monofractions were picked out under a binocular microscope from fractions from +0.25 to –0.5 and from +0.5 to –1.0 mm in size. In most cases we failed to separate ankerite and calcite in their intimate intergrowths. Carbonates were consecutively decomposed in acid at different temperatures. A common charge of ankerite and calcite was broken down in  $\text{H}_3\text{PO}_4$  at 25°C. Afterwards, the residue was heated to 100°C. The obtained gas phases corresponded to calcite and ankerite, respectively. Quartz and hematite were broken down with  $\text{ClF}_3$ . Sulfates assigned for isotopic analysis of sulfur were decomposed with  $\text{V}_2\text{O}_5$ , and sulfides, with  $\text{CuO}$ , using the standard technique. The isotopic compositions were measured on an MI-1201B mass spectrometer. The  $\delta^{18}\text{O}$ ,  $\delta^{13}\text{C}$ , and  $\delta^{34}\text{S}$  values are given in parts per thousand relative to the SMOW, PDB, and Sikhote Alin standards, respectively. The accuracy of  $\delta^{18}\text{O}$  and  $\delta^{13}\text{C}$  determinations was  $\pm 0.2\text{‰}$  and of  $\delta^{34}\text{S}$ ,  $\pm 0.3\text{‰}$ .

#### Rb–Sr SYSTEM AND AGE OF CARBONATITES

To date ankerite–calcite and siderite carbonatites of central Tuva, Rb–Sr mineral isochrons were constructed. In applying this method to the studied rocks, the following specific features should be kept in mind. Mica (Fe-muscovite) is the single (and a low-abundance) high-Rb phase in both types of carbonatites. The reliability of datings calculated from mica–mineral pairs with a low  $^{87}\text{Rb}/^{86}\text{Sr}$  ratio depends on the retention of closed state of the Rb–Sr isotopic system of muscovite after its crystallization. As was mentioned above, carbonatites are commonly altered at the postmagmatic

**Table 1.** Rb and Sr isotopic composition of carbonatites from central Tuva

Mineral	Rb, ppm	Sr, ppm	$^{87}\text{Rb}/^{86}\text{Sr}$	$^{87}\text{Sr}/^{86}\text{Sr}$	$2\sigma$
<i>Ankerite–calcite carbonatite of the Ulatai field (sample Uch-19/5)</i>					
Apatite	1.1	1956	0.0016	0.704347	19
Ankerite	0.04	317	0.0003	0.704703	12
Calcite	0.28	323	0.0025	0.704759	10
Muscovite	211	31	19.66	0.737286	14
Whole-rock sample	6.4	370	0.0499	0.704677	16
<i>Ankerite–calcite carbonatite of the South Choza field (sample Uch-79)</i>					
Apatite	2.4	5932	0.0012	0.704229	18
Calcite colored by iron hydroxides	0.08	100	0.0023	0.705809	19
Newly formed calcite	0.13	25.3	0.0152	0.707381	46
Muscovite	176	15.8	32.12	0.758816	19
Fine-grained quartz–muscovite intergrowths	89	12.5	20.62	0.739814	18
Whole-rock sample	8.9	76.8	0.337	0.706619	18
<i>Ankerite–calcite carbonatite of the Karasug field (sample K-538)</i>					
Whole-rock sample	0.23	1703	0.0004	0.704247	12
<i>Siderite carbonatite of the Karasug field (sample Ks-3/2)</i>					
Fluorite	0	1440	0	0.704157	14
Siderite	0.65	162	0.0116	0.706558	22
Baritocelastine	–	–	–	0.707258	16
Muscovite	389	16.1	70.07	0.822135	21
<i>Siderite carbonatite of the Karasug field (sample K-Hole-1)</i>					
Apatite	4.9	1580	0.009	0.704516	19
Baritocelastine	–	–	–	0.706496	12
Whole-rock sample	4.5	142460	0.0001	0.706316	19

stage. Three samples with different degrees of epigenetic alteration were chosen for analysis: unaltered ankerite–calcite carbonatite from the Ulatai field (sample Uch-19/5), ankerite–calcite carbonatite from the South Choza field severely altered under supergene conditions (sample Uch-79), and siderite carbonatite from the Karasug deposit partly replaced with celestine (sample Ks-3/2). It should be noted that alteration of carbonatites was selective and did not lead to recrystallization or replacement of most rock-forming minerals, including mica and accessory apatite.

The parameters of the Rb–Sr isotopic system were measured in muscovite, accessory apatite, rock-forming carbonates (ankerite, calcite, and siderite), and fluorite phenocrysts. In addition, baritocelastine and newly formed supergene calcite were involved in the study. The measurement results are given in Table 1.

In minerals with low  $^{87}\text{Rb}/^{86}\text{Sr}$  ratio, the  $^{87}\text{Sr}/^{86}\text{Sr}$  value varies in a relatively wide range. In sample Uch-19/5, this value ranges from 0.70435 to 0.70476; in sample Uch-79, from 0.70423 to 0.70738; and in sample Ks-3/2, from 0.70416 to 0.70726. The observed

variation cannot be accounted for only by addition of radiogenic Sr, but is caused by postmagmatic alteration of rocks (see below).

To determine the age, we eliminate the isotopic compositions of minerals with a low  $^{87}\text{Rb}/^{86}\text{Sr}$  ratio from consideration and turn to the Rb–Sr system of muscovites from different samples. The data points for muscovite reveal a correlation in the coordinates  $^{87}\text{Rb}/^{86}\text{Sr}$ – $^{87}\text{Sr}/^{86}\text{Sr}$  (Fig. 8a), and the regression line corresponds to an age of  $118 \pm 9$  Ma. Strictly speaking, this line is not an isochron because muscovites were taken from different carbonatite occurrences and never were in equilibrium, as is reflected in the large MSWD value of 7.5. However, estimates based on micas, as a rule, bear only chronological information because the  $^{87}\text{Rb}/^{86}\text{Sr}$  ratio of micas is high and a large addition of radiogenic Sr conceals the initial heterogeneity of Sr isotopic composition. Because muscovites from different fields give consistent results, the studied samples may be considered coeval and the obtained age estimate may be accepted as the time of carbonatite formation in central Tuva.



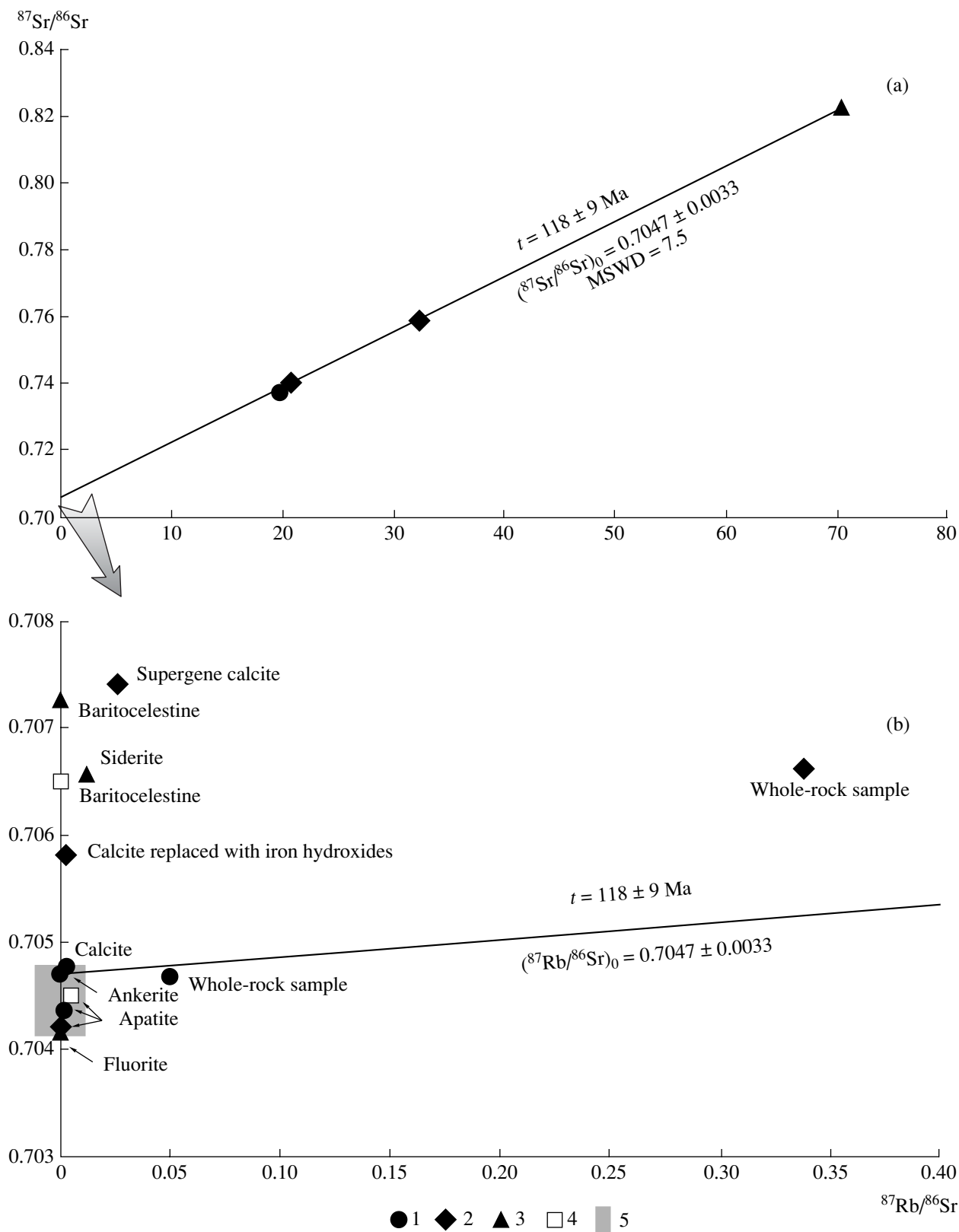


**Fig. 8.** (a) Rb–Sr isochron for micas from carbonatites of central Tuva and (b) isotopic compositions of low-Rb minerals and whole-rock samples. (1, 2) Ankerite–calcite carbonatite from the Ulatai and South Choza fields: (1) sample Uch-19/5, (2) sample Uch-79; (3, 4) siderite carbonatite from the Karasug field: (3) sample Ks-3/2, (4) sample K-Hole-1; (5) field of low-Rb minerals from unaltered carbonatites of central Tuva.

This estimate coincides with the K–Ar age of mica from greisenized and hydrothermally altered granites in the Karasug deposit: 124, 122, and 114 Ma (Shurupov et al., 1966).

Let us specify the initial Sr isotopic composition of carbonatites because the initial  $^{87}\text{Sr}/^{86}\text{Sr}$  ratio obtained from the regional mica isochron ( $0.7047 \pm 33$ ) is too uncertain. The Sr isotopic compositions of minerals with a low Rb/Sr ratio are within a very wide range from 0.70416 to 0.70726 both in particular samples and in the entire set of carbonatite samples (Fig. 8b). As was mentioned above, the modal composition of carbonatites was formed during several stages. Carbonates, fluorite, mica, and apatite pertain to the primary mineral assemblage formed as a result of magmatic crystallization of carbonatites. While mica and apatite do not bear indications of postmagmatic and supergene alterations, such indications are observed rather distinctly in carbonates and fluorite.

The Sr isotopic compositions of apatites from the Karasug, Ulatai, and South Choza fields are close to one another (Table 1). Apatite from ankerite–calcite carbonatite has  $^{87}\text{Sr}/^{86}\text{Sr} = 0.70435$  (sample Uch-19/5) and 0.70423 (sample Uch-79); siderite carbonatite has  $^{87}\text{Sr}/^{86}\text{Sr} = 0.70452$  (sample K-Hole-1). The Sr isotope ratio of fluorite from siderite carbonatite of the Karasug deposit (sample Ks-3/2) equals 0.70416 and is close to the above values. The whole-rock sample K-538 of unaltered ankerite–calcite carbonatite from the Karasug field was taken from a borehole core at a depth of 372 m below the oxidation zone; for this sample,  $^{87}\text{Sr}/^{86}\text{Sr} = 0.70425$ . The Sr isotope ratios of calcite and ankerite from the slightly altered (under supergene conditions) carbonatite in the Ulatai field (sample Uch-19/5) are almost equal (0.70470 and 0.70476, respectively) and somewhat higher than that of apatite from the same sample (0.70435). Most likely, the  $^{87}\text{Sr}/^{86}\text{Sr}$  values within the range from 0.70416 to 0.70476 are close to the initial Sr isotope ratio of carbonatites.

The Sr isotope ratios of other analyzed minerals from both carbonatite varieties—hydrothermal baritocelastine, recrystallized calcite, and newly formed supergene calcite—are systematically higher than the suggested initial  $^{87}\text{Sr}/^{86}\text{Sr}$  ratio of carbonatites (Fig. 8b) as a result of epigenetic alteration.

The studied samples of siderite carbonatites at the Karasug deposit (Ks-3/2 and K-Hole-1) were taken from borehole cores that were not affected by supergene alteration. The replacement of primary barite with hydrothermal baritocelastine is the main process of alteration of these carbonatites. Baritocelastine from both samples has a high  $^{87}\text{Sr}/^{86}\text{Sr}$  ratio equal to 0.70726 and 0.70650. These values are sharply distinct from the Sr isotopic compositions of fluorite and apatite from the same samples (Fig. 8b). The  $^{87}\text{Sr}/^{86}\text{Sr}$  ratio of siderite from sample Ks-3/2 is also high (0.70656). Thus, it may be suggested that a source of celestine enriched in radiogenic Sr was involved.

The Sr isotopic composition also changed as a result of supergene alteration. The studied samples represent rocks affected by this process with different intensity. Whole-rock sample K-538 from unaltered ankerite–calcite carbonatite taken from a depth of 372 m in the Karasug field is characterized by a high Sr content (1700 ppm) and a low  $^{87}\text{Sr}/^{86}\text{Sr}$  ratio of 0.70425. In calcite and ankerite from slightly altered carbonatites of the Ulatai field (sample Uch-19/5), the Sr contents are similar (~320 ppm); the  $^{87}\text{Sr}/^{86}\text{Sr}$  values are almost identical (0.70470 and 0.70476) and only insignificantly differ from that of apatite from the same sample (0.70435). Sample Uch-79 of carbonatite from the South Choza field was taken from intensely altered rock. Ankerite is completely replaced with iron hydroxides and calcite; pockets and stringers of the newly formed supergene calcite are observed throughout the rock. The  $^{87}\text{Sr}/^{86}\text{Sr}$  ratio of brown calcite colored by iron hydroxides is elevated (0.70581) in comparison with primary calcite in sample Uch-19/5, while the Sr content is lowered (100 ppm). This tendency is expressed most clearly in the composition of supergene calcite from the same rock, which contains only 25 ppm Sr, while its  $^{87}\text{Sr}/^{86}\text{Sr}$  ratio reaches a maximum (0.70738). Thus, the supergene alteration of ankerite–calcite carbonatites lead to the depletion of rock-forming carbonates in Sr and to an increase in the  $^{87}\text{Sr}/^{86}\text{Sr}$  ratio. In other words, the process was accompanied by removal of Sr and isotopic exchange with alien Sr, e.g., with this element contained in the country rocks.

Thus, the isotopic Rb–Sr study of whole-rock samples and minerals of ankerite–calcite and siderite carbonatites of central Tuva has shown that  $^{87}\text{Sr}/^{86}\text{Sr}$  ratios in primary minerals unaltered by postmagmatic processes lie within a rather narrow range of 0.70416–0.70476. Even the highest value does not come into conflict with the suggestion on the mantle source of carbonatites. During the postmagmatic period, the Sr isotopic composition of carbonatites changed, largely owing to the involvement of sources enriched in radiogenic Sr in the process of hydrothermal celestinization and supergene alteration. The country rocks and the related connate water could have served as such sources. The  $^{87}\text{Sr}/^{86}\text{Sr}$  ratio for these sources may be deduced from the data reported by Blokh and Dagaeva (1987); they assessed the  $^{87}\text{Sr}/^{86}\text{Sr}$  value of sulfates from sedimentary fill of the Tuva Trough and its framework at 0.7062–0.7072.

## OXYGEN AND CARBON ISOTOPIC COMPOSITIONS

Two main goals were pursued in the choice of samples for isotopic study: characterizing the primary isotopic composition of carbonatites and determining its modification related to the supergene oxidation of rocks. The following materials served as objects for isotopic analysis of carbon and oxygen: (1) primary anker-

ite–calcite carbonatites from different fields (calcite and ankerite monofractions and whole-rock samples), both unoxidized and oxidized to various degrees; (2) secondary calcite from ankerite–calcite carbonatites newly formed under supergene conditions; (3) unoxidized and partly oxidized siderite carbonatites from the Karasug and Ulatai fields (siderite monofractions and whole-rock samples); (4) primary quartz phenocrysts from siderite and ankerite–calcite carbonatites; (5) tabular hematite (specularite) from carbonatites; (6) carbonates from older quartz–carbonate veins; and (7) strontianite and calcite from late veinlets in the oxidation zone of carbonatites at the Karasug deposit. The analytical results and characteristics of samples are represented in Tables 2 and 3. Previous determinations performed in 1983 at the Institute of Geophysics and Physics of Minerals in Kiev and in 1986 and 1991 at the Institute of the Lithosphere in Moscow were supplemented; these data were partly published by Bolonin and Zhukov (1983).

#### *Oxygen and Carbon Isotopic Compositions of Ankerite–Calcite Carbonatites*

The carbon and oxygen isotopic compositions of rock-forming carbonates unaltered under supergene conditions from the Karasug, Teeli–Orgudyd, Ulatai, and South Choza fields are rather close to one another:  $\delta^{13}\text{C}$  ranges from  $-3.7$  to  $-4.9\text{‰}$  and  $\delta^{18}\text{O}$ , from  $+8.8$  to  $+13.8\text{‰}$  (Table 2, Fig. 9). The isotopic compositions of ankerite and calcite from the same samples (Fig. 9, I, II, V, VI) demonstrate a smaller scatter, and calcite is commonly enriched in  $^{18}\text{O}$  relative to the associated ankerite by  $1.3$ – $2.2\text{‰}$  (Table 2, nos. 5–8, 27, 28, 31, 32). The available partition coefficients (Zheng, 1999) indicate that, at the equilibrium crystallization of these minerals, the  $^{18}\text{O}$  distribution should be the reverse. A low content of an Mg admixture in calcite (no higher than  $0.1$  wt %) is inconsistent with its paragenesis with ankerite (Bolonin and Nikiforov, 2004) and confirms the nonequilibrium between these minerals. Thus, despite the absence of obvious corrosion relationships between ankerite and calcite, it may be suggested that they were not formed simultaneously and the mineral-forming medium was evolving during crystallization of carbonates.

Under supergene conditions, the O and C isotopic composition changed, with these changes being greater the more intense the rock transformation. Carbonatite samples Uch-18 and Uch-19/3 from the Ulatai field represent rocks at the very beginning stage of supergene alteration, which affected only separate ankerite crystals along sporadic fractures. Both unoxidized ankerite and its crystals with iron hydroxides in association with tiny segregations of calcite newly formed along grain boundaries and cleavage planes were analyzed. While the shift of the carbon isotopic composition of partially altered ankerite and newly formed calcite (Fig. 9, arrows in V, VI) is insignificant and remains

within the analytical uncertainty, oxygen is enriched in the heavy isotope approximately by  $1.5\text{‰}$  (Table 2, nos. 29, 30, 33).

Severely altered ankerite–calcite carbonatite, where ankerite is partially or completely replaced with iron hydroxides and secondary calcite and primary calcite is partly recrystallized, is characterized by appreciable enrichment in the heavy oxygen isotope. Extremely oxidized carbonatite (sample Uch-27) transformed into highly porous, almost loose limonite–calcite rock has  $\delta^{18}\text{O} = +19.2\text{‰}$  (Table 2, no. 34). Calcite formed under supergene conditions in axial zones of recrystallization is most enriched in  $^{18}\text{O}$ , up to  $+22\text{‰}$  (Fig. 9; Table 2, nos. 36, 43, 49, 56). The variation of carbon isotopic composition does not have a systematic character: in some cases, the isotopic composition remains unchanged and in others it is enriched in  $^{13}\text{C}$ .

The isotopic characteristics of carbonatites from the Chaakhol field differ from those of ankerite–calcite carbonatites in other fields of central Tuva (Table 2, nos. 51–53; Fig. 9b). Carbonates in all samples are enriched in  $^{13}\text{C}$ :  $\delta^{13}\text{C}$  varies from  $-1.5$  to  $-3.2\text{‰}$ . Minerals of unoxidized carbonatites from thin veins are depleted in  $^{18}\text{O}$  ( $\delta^{18}\text{O} = 5.5$ – $6.8\text{‰}$ ). Carbon and oxygen isotopic compositions of ankerite and calcite from sample Chkh-4, which represents rock at the initial stage of supergene alteration, correspond to the ranges of ankerite–calcite carbonatites from other fields. Similar O and C isotopic compositions are inherent to transparent crystals of the newly formed calcite from this sample (Table 2, nos. 54–56).

The oxygen isotopic composition of dipyrimal crystals of primary quartz from ankerite–calcite carbonatites pertaining to various fields, the Chaakhol field included, yields similar values ( $\delta^{18}\text{O} = 11.6$ – $13.7\text{‰}$ ) irrespective of the degree of supergene alteration (Table 3, Fig. 9).

The postmagmatic alteration of ankerite–calcite carbonatites is locally accompanied by crystallization of hematite metacrysts without recrystallization of rock-forming carbonates. No difference in oxygen isotopic composition was established between hematite-bearing sample Uch-18 (Fig. 9, VI) and sample Uch-19/3 (Fig. 9, V), devoid of hematite. If it is assumed that hematite was formed at isotopic equilibrium with replaced carbonates, the isotopic geothermometers (Zheng and Simon, 1991; Zheng, 1999) yield  $380 \pm 20^\circ\text{C}$  ( $\Delta\delta^{18}\text{O} = 13.4\text{‰}$ ) for the calcite–hematite pair and  $440 \pm 20^\circ\text{C}$  ( $\Delta\delta^{18}\text{O} = 12.1\text{‰}$ ) for the ankerite–hematite pair from sample Uch-18.

#### *Oxygen and Carbon Isotopic Compositions of Siderite Carbonatites*

Samples of unoxidized siderite carbonatite were available only for the Karasug field. This porphyritic rock consists of large (2–20 mm) siderite rhombohe-

**Table 2.** Oxygen and carbon isotopic compositions of whole-rock samples and minerals of carbonatites from central Tuva

No.	Mineral type	Sample and their location	Material	Degree of oxidation of minerals and rocks	$\delta^{18}\text{O}$ , ‰ SMOW	$\delta^{13}\text{C}$ , ‰ PDB
<i>Karasug field</i>						
1	Ankerite–calcite carbonatite	Hole 535, 232 m	Whole-rock sample	–	10.6	–4.7
2		Hole 537, 231 m	"	–	12.0	–3.7
3		Hole 538, 341 m	"	–	14.7	–3.6
4		K-52, surface	Calcite	++	13.2	–4.4
5		Hole 538, 372 m	"	–	13.1	–4.3
6			Ankerite	–	10.5	–4.6
7		Hole 535, 273 m	Calcite	–	11.2	–4.2
8			Ankerite	–	8.8	–4.9
9	Siderite carbonatite	Hole 529, 158 m	Siderite phenocrysts	–	10.9	–3.9
10			Siderite from ground-mass	–	12.0	–4.6
11		Hole 529, 136 m	Whole-rock sample	–	12.4	–4.2
12		K-56, surface	Siderite	+	9.9	–5.8
13		K-Hole-1	"	–	9.2	–4.5
14		Ks-4/5, hole	Siderite phenocrysts	–	11.0	–5.9
15			Siderite phenocrysts	+	10.6	–6.5
16		Siderite from ground-mass	–	12.1	–5.3	
17	Hydrothermal quartz–carbonate veins	Shaft 1	Calcite	–	16.4	–4.8
18			"	–	15.4	–3.9
19			Ankerite	–	16.3	–4.9
20	Veinlets in oxidation zone of carbonatite	Adit 6, inset 2a	Yellow strontianite	–	17.3	–3.3
21			White strontianite	–	18.2	–3.9
22		K-50, surface	Pink strontianite	–	17.0	–4.5
23		3-rt, surface	Brown calcite	–	20.0	–4.1
<i>Ulatai field, samples from surface</i>						
24	Ankerite–calcite carbonatite	23	Whole-rock sample	–	10.4	–4.1
25		13a	"	–	11.3	–4.1
26		21-88	"	+	13.4	–4.7
27			Ankerite	–	10.2	–4.5
28		Uch-18	Calcite	–	11.5	–4.4
29			Ankerite	+	11.9	–4.2
30	Calcite after ankerite		+++	13.3	–4.3	

**Table 2.** (Contd.)

No.	Mineral type	Sample and their location	Material	Degree of oxidation of minerals and rocks	$\delta^{18}\text{O}$ , ‰ SMOW	$\delta^{13}\text{C}$ , ‰ PDB
<i>Ulatai field, samples from surface</i>						
31	Ankerite–calcite carbonatite	Uch-19/3	Ankerite	–	9.8	–3.7
32			Calcite	–	11.4	–3.7
33			Calcite after ankerite	+++	13.1	–3.5
34		Uch-27	Calcite	++	19.2	–0.9
35		Uch-31	"	++	19.5	–1.6
36				Newly formed calcite	+++	21.7
37	Siderite carbonatite	Uch-21	Siderite	+	16.7	–2.2
38			Calcite after ankerite	+++	17.1	–2.0
<i>Teeli–Orgudyd field, samples from surface</i>						
39	Ankerite–calcite carbonatite	Uch-47	Ankerite	–	13.8	–4.8
40			Calcite	–	12.3	–4.7
41		Uch-48	"	++	15.0	–3.5
42			Ankerite	++	15.0	–3.7
43			Newly formed calcite	+++	19.1	–3.2
<i>South Choza field, samples from surface</i>						
44	Ankerite–calcite carbonatite	Yuch-1	Whole-rock sample	++	13.2	–6.0
45		Yuch-2	"	++	15.9	–5.9
46		Yuch-3	"	++	19.1	–5.5
47		Uch-79	Calcite	++	19.1	–4.8
48			Ankerite	++	17.1	–5.5
49			Newly formed calcite	+++	22.1	–4.9
50		Uch-82	Calcite	++	17.1	–4.7
<i>Chaakhol field</i>						
51	Ankerite–calcite carbonatite	Chkh-1, Hole 702	Calcite	–	5.5	–3.2
52		Chkh-3, Hole 704	Ankerite	–	6.8	–1.5
53			Calcite	–	6.6	–1.8
54		Chkh-4, surface	Ankerite	+	12.2	–2.3
55			Calcite	+	12.8	–2.4
56			Newly formed calcite	+++	12.8	–2.8
57	Hydrothermal quartz–carbonate veins	Chkh 9/3, Hole 704	Calcite	–	19.5	–3.3

Note: (–) indications of oxidation are absent; (+) admixture of iron hydroxides, <1–2%; (++) admixture of iron hydroxides, 2–20%; (+++) secondary calcite, including newly formed variety and pseudomorphs after oxidized ankerite and siderite. Analyses were performed at the Geological Institute, RAS (samples 4–8, 12–16, 22, 27–43, 47–57); the Institute of the Lithosphere, RAS (samples 1, 24–26, 44–46); and the Institute of Geophysics and Physics of Minerals, Academy of Sciences of the Ukrainian SSR (samples 2, 3, 9–11, 17–21, 23).

drons and phenocrysts of fluorite, barite, quartz, and pyrite incorporated into a fine-grained (<0.2 mm) fluorite–siderite groundmass. In two samples, the isotopic compositions were determined separately for siderite monofractions from phenocrysts and the groundmass (Fig. 9, *PhC* and *GM*, respectively). In both samples, the difference between *PhC* and *GM* turned out to be beyond the uncertainty limits (Fig. 9a, III, IV). This indicates that the mineral-forming medium changed during crystallization of phenocrysts and the matrix. However, a different shift of carbon isotopic composition (toward enrichment and depletion in  $^{13}\text{C}$ ) in the samples does not allow us to consider degassing as a single cause of such variations. The involvement of alien O and C sources, e.g., groundwater or carbonate material of country rocks, cannot be ruled out.

Siderite carbonatite is readily oxidized under supergene conditions and replaced with iron hydroxides, occasionally in association with calcite. Two samples of borehole cores characterize the initial stage of oxidation; thereby, in sample Ks-4/5 (Fig. 9a, IV), iron hydroxides replace siderite only in sporadic grains. Oxygen and carbon isotopic compositions in unaltered and oxidized siderite phenocrysts are different (Table 2, nos. 14, 15). The isotopic compositions of siderite in sample Uch-21 from the Ulatai field (Table 2, no. 37), where siderite is not completely oxidized, are close to those of supergene calcite from the same sample.

The oxygen isotopic compositions of dipyrimid crystals of primary quartz from two samples of siderite carbonatites from the Karasug and Ulatai fields are almost the same,  $\delta^{18}\text{O} = +11.2$  and  $+11.4\%$  (Table 3), and virtually coincide with the average oxygen isotopic compositions of unoxidized siderite carbonatite from the Karasug field and of quartz from ankerite–calcite carbonatite (Fig. 9).

#### Oxygen and Carbon Isotopic Compositions of Veinlets

Strontianite from veinlets in carbonatite bodies of the Karasug field is almost identical in carbon isotopic composition to primary carbonatite (Fig. 9a). At the same time, oxygen in strontianite, as in carbonatites altered under supergene conditions, is enriched in  $^{18}\text{O}$  up to  $18\%$ . In veins of brown calcite colored by iron hydroxides and associated with strontianite veinlets,  $\delta^{18}\text{O} = +20\%$  (Fig. 9a).

Thin quartz-carbonate veins that cut terrigenous rocks in carbonatite fields predated carbonatite formation, and fragments of these rocks are found in carbonatites. Oxygen and carbon isotopic compositions of ankerite and calcite from older veins in the Karasug and Chaakhol fields clearly differ from those of primary carbonatites, first of all, by oxygen (Fig. 9).

**Table 3.** Oxygen isotopic composition of quartz and hematite from carbonatites of central Tuva

Rock type	Carbonatite field	Sample	$\delta^{18}\text{O}, \%$
<i>Quartz</i>			
Ankerite–calcite carbonatite	Teeli–Orgudyd	Uch-47	11.6
	Chaakhol	Chkh-4	13.0
Oxidized ankerite–calcite carbonatite	South Choza	Uch-79	12.1
	Ulatai	Uch-27	13.7
Siderite carbonatite	Karasug	K-56	11.2
Oxidized siderite carbonatite	Ulatai	Uch-32	11.4
<i>Hematite</i>			
Ankerite–calcite carbonatite	Ulatai	Uch-18	–1.9
Oxidized ankerite–calcite carbonatite	South Choza	Uch-79	–0.1
Oxidized siderite carbonatite	Karasug	K-3	–0.6

Note: Analyses were performed at the Geological Institute, RAS.

#### SULFUR ISOTOPIC COMPOSITION

The sulfur isotopic composition was determined in (1) pyrite phenocrysts from primary siderite and ankerite–calcite carbonatites, (2) primary barite from siderite carbonatite, (3) epigenetic hydrothermal sulfates (baritocelastine and celestine) as pseudomorphs after primary barite, and (4) pyrite metacrysts in country rocks. The results of the isotopic study are presented in Table 4 and shown in Fig. 10.

Pyrite from ankerite–calcite carbonatite with  $\delta^{34}\text{S} = +0.3$  and  $+1.1\%$  differs from pyrite associated with barite in siderite carbonatite with  $\delta^{34}\text{S} = -1.8, -2.6, -2.8,$  and  $-4.4\%$ . Since no sulfates are known in ankerite–calcite carbonatite, it may be expected that the isotopic composition of sulfide sulfur in this carbonatite did not change in the process of mineral formation and corresponds to that of a carbonatitic magma source. Pyrite and barite that coexist in siderite carbonatite likely contain sulfur that underwent isotopic fractionation between sulfide and sulfate species. Pyrite is enriched in the light sulfur isotope, and barite in the heavy isotope ( $\delta^{34}\text{S}$  varies from  $+8.6$  to  $+9.7\%$ ). If pyrite and barite are in isotopic equilibrium, then the average difference in  $\delta^{34}\text{S}$  of  $12\%$  corresponds to a temperature of  $530^\circ\text{C}$  (Ohmoto and Rye, 1979). This estimate is lower than the homogenization temperature of brine–melt inclusions in fluorite from carbonatite, which reaches  $660\text{--}750^\circ\text{C}$  (Kandinov and Kharlamov, 1978). A cause of the discrepancy may be asynchronous crystallization of pyrite and barite. These minerals do not make up intergrowths, and, as judged from the



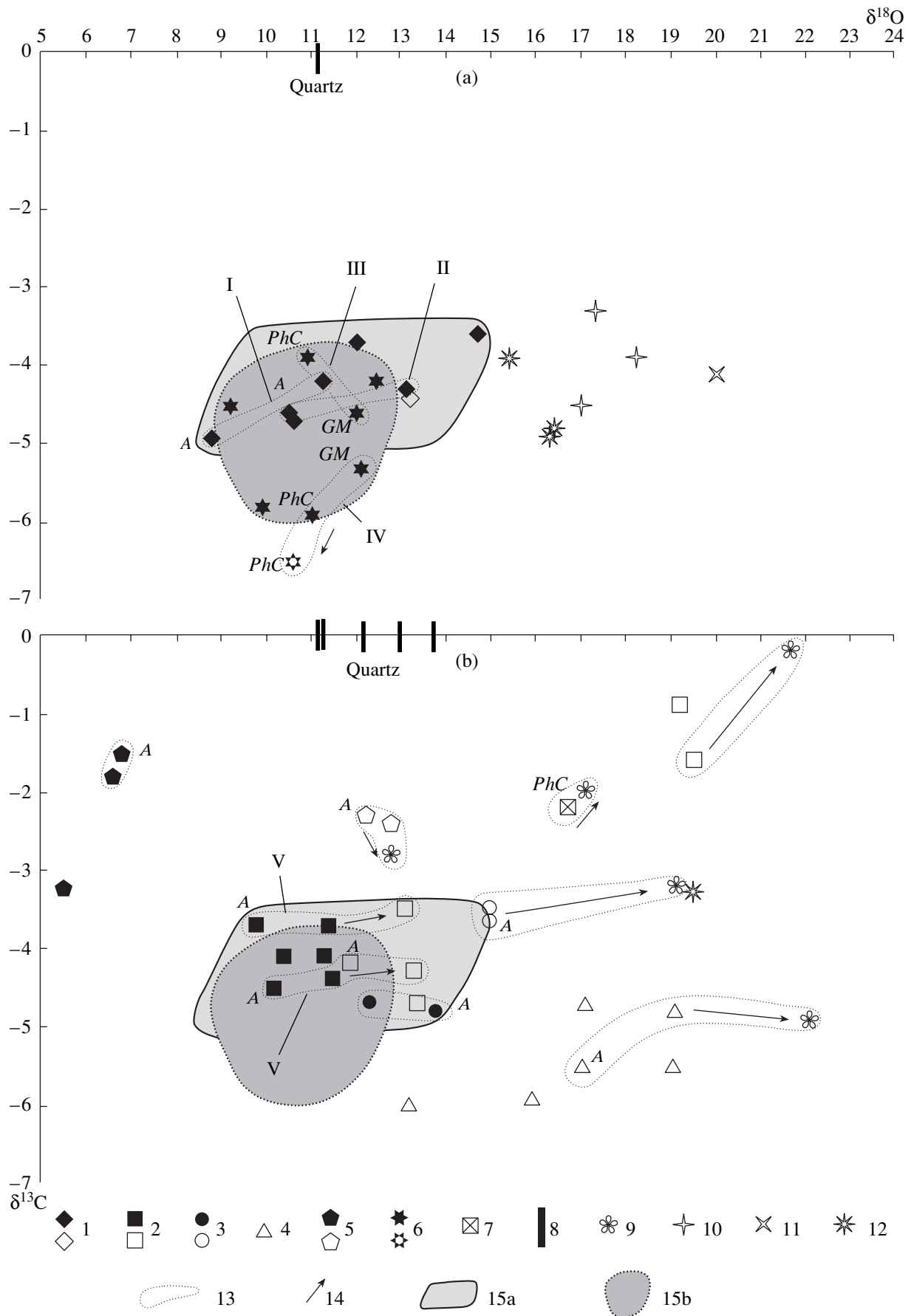


**Fig. 9.** Oxygen and carbon isotopic compositions of carbonatites and related minerals from central Tuva. (a) Karasug field, (b) Chaakhoh, Teeli–Orgudyd, Ulatai, and South Choza carbonatite fields. Filled symbols are carbonatites without indications of postmagmatic and supergene alteration; open symbols are carbonatites with indications of supergene alteration (admixture of iron hydroxides). (1–5) Carbonate from ankerite–calcite carbonatites of the (1) Karasug, (2) Ulatai, (3) Teeli–Orgudyd, (4) South Choza, and (5) Chaakhoh fields; (6, 7) siderite from siderite carbonatite of the (6) Karasug and (7) Ulatai fields; (8) quartz as faceted phenocrysts scattered in carbonate matrix; (9) calcite newly formed under supergene conditions in recrystallized carbonatites; (10, 11) veinlets in oxidation zone of carbonatites in the Karasug field; (10) strontianite, (11) brown calcite; (12) ankerite and calcite from hydrothermal quartz–carbonate veins in country rocks; (13) minerals from one sample (I–VI, see text for explanation): (A) ankerite, (PhC) siderite phenocrysts, (GM) siderite from groundmass; other symbols within contours are calcite; (14) variation of isotopic compositions of minerals from one sample in the course of supergene alteration; (15) generalized fields of (a) ankerite–calcite and (b) siderite carbonatites from central Tuva except for carbonatites of the Chaakhoh field.

frequent corrosion of pyrite grains, its crystallization predated the formation of barite.

Siderite carbonatite contains 1.3 wt % of sulfide sulfur ( $S^{2-}$ ) and 2.2 wt % of sulfate sulfur ( $S^{4+}$ ), on average; the  $\delta^{34}S$  values are  $-2.9$  and  $+9.2\text{‰}$ , respectively. On the basis of these data, one may calculate the weighted average bulk isotopic composition of sulfur in this carbonatite  $(-2.9\text{‰} \times 1.3 + 9.2\text{‰} \times 2.2)/3.5 = +4.7\text{‰}$ . This estimate substantially deviates from the suggested primary  $\delta^{34}S = +(0.3-1.1)\text{‰}$  recorded in pyrite from ankerite–calcite carbonatite. Such a deviation may be accounted for by removal of isotopically light sulfur in the form of  $SO_2$  as a result of intense

degassing under a high oxygen fugacity (Sakai et al., 1982).

Epigenetic hydrothermal sulfates (pseudomorphs of baritocelastine and celestine after primary barite) reveal an elevated  $\delta^{34}S$  varying from  $+9.0$  to  $+14.5\text{‰}$ . They inherit the sulfur isotopic composition of primary barite and become enriched in the heavy isotope derived from an outer source. In contrast to the S isotopic composition of primary barite from carbonatites of the Karasug field, barite from siderite carbonatites of the Chaakhoh and Ulatai fields altered under supergene conditions is also enriched in heavy sulfur up to  $\delta^{34}S = +14.5$  and  $+14.4\text{‰}$ , respectively.

**Table 4.** Sulfur isotopic composition of pyrite and sulfates

Rock type	Sample	Carbonatite field	Material	$\delta^{34}S, \text{‰}$
<i>Pyrite</i>				
Ankerite–calcite carbonatite	Uch-18	Ulatai	Pyrite phenocrysts	+0.3
	Chkh-4	Chaakhoh		+1.1
Siderite carbonatite	K-Hole-1	Karasug	Pyrite phenocrysts	-1.8
	*			-2.6
	*			-2.8
	*			-4.4
Metasomatically altered gravelstone	Uch-75	North Choza	Pyrite metacrysts	+8.9
<i>Sulfates</i>				
Siderite carbonatite	*	Karasug	Barite phenocrysts	+8.6
	*			+9.7
	K-3		Baritocelastine pseudomorph after barite	+9.6
	*			+10.2
	K-56			+12.3
	K-Hole-1		Celestine pseudomorph after barite	+14.5
	*			+9.0
	Uch-21			Ulatai
Chkh-6	Chaakhoh	+14.5		

\* Analyses were performed at the Institute of Geophysics and Physics of Minerals, Academy of Sciences of the Ukrainian SSR (MI-1309 mass spectrometer, accuracy  $\pm 0.2\text{‰}$ , analysts Z.N. Kravchuk and V.I. Vlasenko, 1983); other samples were analyzed at the Geological Institute, RAS.

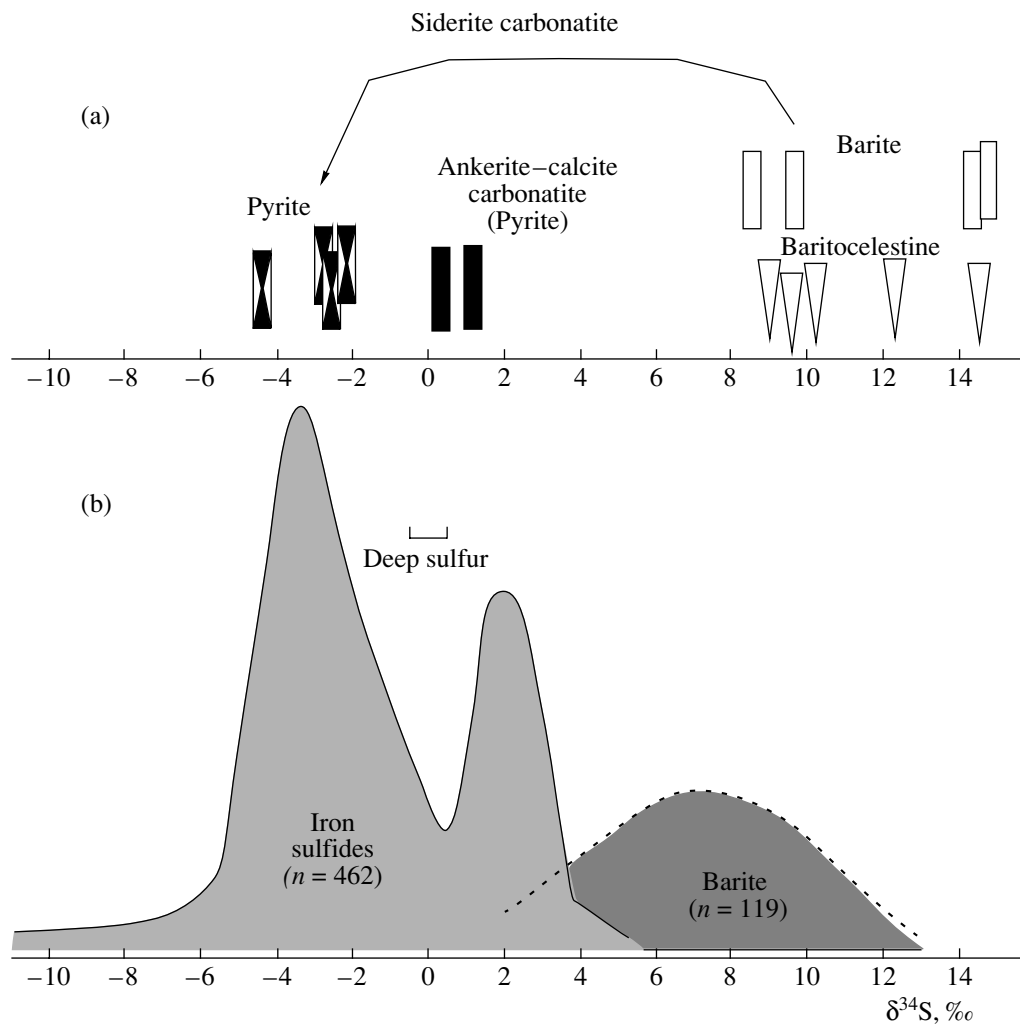


**Fig. 10.** Sulfur isotopic composition of iron sulfides and sulfates from carbonatites of (a) central Tuva and (b) other provinces, after Deines (1989). Isotopic composition of deep sulfur is given after Sakai et al. (1984) and Taylor (1986).

On the basis of representative statistical data (462 analyses), Deines (1989) showed that pyrite and pyrrhotite from carbonatites of various provinces reveal a bimodal distribution of  $\delta^{34}\text{S}$ . One peak falls within the range  $+1\text{--}3\text{‰}$ , and the other, within the range from  $-1.5\text{--}5\text{‰}$  (Fig. 10). Both maxima differ from the isotopic composition of “deep” sulfur ( $\delta^{34}\text{S} = 0 \pm 0.5\text{‰}$ ) in meteorites and fresh MORB glasses (Sakai et al., 1984; Taylor, 1986). Sulfates (more than 119 samples of barite and baritocelastine from various provinces in the selection presented by Deines (1989)) are enriched in the heavy isotope and  $\delta^{34}\text{S}$  ranges from  $+2$  to  $+12\text{‰}$  (Fig. 10). Thus, the sulfur isotopic compositions of primary pyrite and barite from the studied Tuvan carbonatites fit the worldwide statistical estimates for such rocks.

## DISCUSSION

The analysis of stable isotopes and the Sr isotopic composition in rocks and minerals is aimed at determi-

nation of their sources. As was mentioned above, ankerite-calcite and siderite carbonatites of central Tuva were formed as products of two-phase injections of brines-melts into fault zones. After solidification, carbonatites were affected by endogenic hematitization, celestinization, and intense supergene alteration, which shifted the isotopic compositions relative to their primary values. The analysis of carefully selected monofractions of minerals belonging to different paragenetic assemblages allowed us to specify the effects of the epigenetic processes on isotopic compositions of carbonatites.

The effect of hematitization was assessed for ankerite-calcite carbonatites in the Ulatai field. The oxygen and carbon isotopic compositions of carbonates in samples with and without hematite turned out to be almost identical. The formation of hematite probably was not related to a foreign source of oxygen, and this mineral was formed in isotopic equilibrium with replaced carbonates at  $380\text{--}440^\circ\text{C}$ .

The formation of hydrothermal celestine and baritocelastine was established only for some siderite carbonatite bodies in the Karasug field. Baritocelastine drastically differs in Sr isotopic composition ( $^{87}\text{Sr}/^{86}\text{Sr} = 0.70650\text{--}0.70726$ ) from fluorite and apatite of preceding assemblages ( $^{87}\text{Sr}/^{86}\text{Sr} = 0.70416\text{--}0.70452$ ). The sulfur isotopic compositions of barite ( $\delta^{34}\text{S} = +8.6$  and  $+9.1\%$ ) and baritocelastine ( $\delta^{34}\text{S} = +9.6$  and  $+14.5\%$ ) are also different. The results obtained indicate that an additional source of the late solutions responsible for celestinization of siderite carbonatites had distinct isotopic parameters.

The supergene alteration widespread at the upper levels of carbonatite bodies in central Tuva substantially changed the oxygen and carbon isotopic compositions in comparison with their initial values. Even an insignificant alteration recorded in a small amount of iron hydroxides replacing ankerite or siderite is accompanied by a shift of the isotopic compositions of carbonates. Primarily, they are enriched in the heavy oxygen isotope.  $\delta^{18}\text{O}$  in highly altered carbonatite reaches  $+19.5\%$ . The shift of the carbon isotopic composition in such rocks is commonly not systematic or is not detected at all. The Sr isotopic composition of carbonates also changed owing to supergene alteration. The recrystallized and newly formed carbonates in altered ankerite–calcite carbonatites stand out by much higher  $^{87}\text{Sr}/^{86}\text{Sr}$  values, up to 0.70738.

Thus, an alien material was gained in the course of supergene alteration and the isotopic compositions of carbonatite became a mixture of materials derived from at least two sources.

Ruling out minerals and whole-rock samples of carbonatites that underwent epigenetic alteration, common regions of O, C, S, and Sr isotopic compositions may be outlined for carbonatites from the Karasug, Ulatai, Teeli–Orgudyd, and South Choza fields (Figs. 8–10). Some specific features distinguish the O and C isotopic compositions of carbonates from the Chaakhol field, while the isotopic compositions of oxygen in quartz and sulfur in pyrite fit the ranges established for carbonatites from other fields. Similar isotopic compositions of studied elements contained in ankerite–calcite and siderite carbonatites allow us to suggest their common source, and this suggestion is supported by their geochemical commonness.

The estimated isotopic characteristics of primary carbonatites reveal heterogeneity, which is recorded even in minerals from the same sample. For example, the O and C isotopic compositions of primary minerals from any sample of ankerite–calcite carbonatite (ankerite, calcite, quartz) or siderite carbonatite (siderite from phenocrysts and the groundmass), being close to one another, do not fit the strict isotopic equilibrium. It may be inferred that minerals crystallized under conditions of variable isotopic composition of carbonatitic melt. A cause of such variation could have been related to degassing or fractionation of melts that disturbed the

equilibrium between the previously formed phenocrysts and the residual melt. Degassing at the temperature typical of carbonatitic liquid results in enrichment of melt in  $^{18}\text{O}$  and  $^{12}\text{C}$  (Hay and O'Neil, 1983). During the melt fractionation, the liquid phase is enriched in  $^{18}\text{O}$  and  $^{13}\text{C}$  (Deines, 1989). However, carbonatites of central Tuva do not furnish direct evidence for rock crystallization from different batches of melt that underwent variable degrees of degassing or mineral fractionation.

The crustal contamination of melts may be another cause of compositional modification of melt during its ascent and residence in transitional and final magma chambers. Carbonatites of central Tuva are hosted in aluminosilicate terrigenous rocks. Their fragments may be found in every carbonatite body. However, carbonatites do not exert appreciable chemical effects on these fragments (Nikiforov et al., 2005). The amount of assimilated fragments of country rocks is insignificant. Quartz and muscovite are the sole silicate minerals in carbonatites, and their total content does not exceed 2–4 vol %. This figure constrains the possible volume of assimilated aluminosilicate material.

The melt also could have assimilated country carbonate rocks and groundwater at a depth. Such assimilation would hardly have changed considerably the bulk chemical composition of carbonatites but could have shifted their isotopic characteristics. Carbonates serve as a cement in some Middle Paleozoic sandstones. Thick (up to 300 m) members of marmorized limestone occur in the Vendian–Cambrian basement of the Tuva Trough. The expected variations of oxygen and carbon isotopic compositions caused by carbonate assimilation will be directed toward simultaneous enrichment of melts in both  $^{13}\text{C}$  and  $^{18}\text{O}$  (Deines, 1989). It should be kept in mind that carbonatitic melt with high C and O contents would serve as a powerful buffer that limits the variation of isotopic compositions of these elements. Mixing of high-temperature ( $>500^\circ\text{C}$ ) melts with metamorphic, formational, or meteoric waters may be realized in various ways (Pokrovsky, 2000). Oxygen is the only element contained in carbonatites and groundwater in commensurable amounts, and therefore the expected shifts in carbonatite isotopic composition caused by their mixing will concern mainly oxygen, the more so as the most significant variations of isotopic compositions of primary minerals from carbonatites of central Tuva are related to this element. The assimilation of groundwater by carbonatitic melt appears preferential in comparison with the assimilation of country carbonate rocks, which would shift the isotopic compositions of both oxygen and carbon.

The variation of initial  $^{87}\text{Sr}/^{86}\text{Sr}$  ratio in primary minerals of carbonatites within the range 0.7042–0.7048 also does not come into conflict with the suggestion on crustal contamination, but at the same time constrains the scale of this process by a narrow range. This limitation follows from the small range of varia-

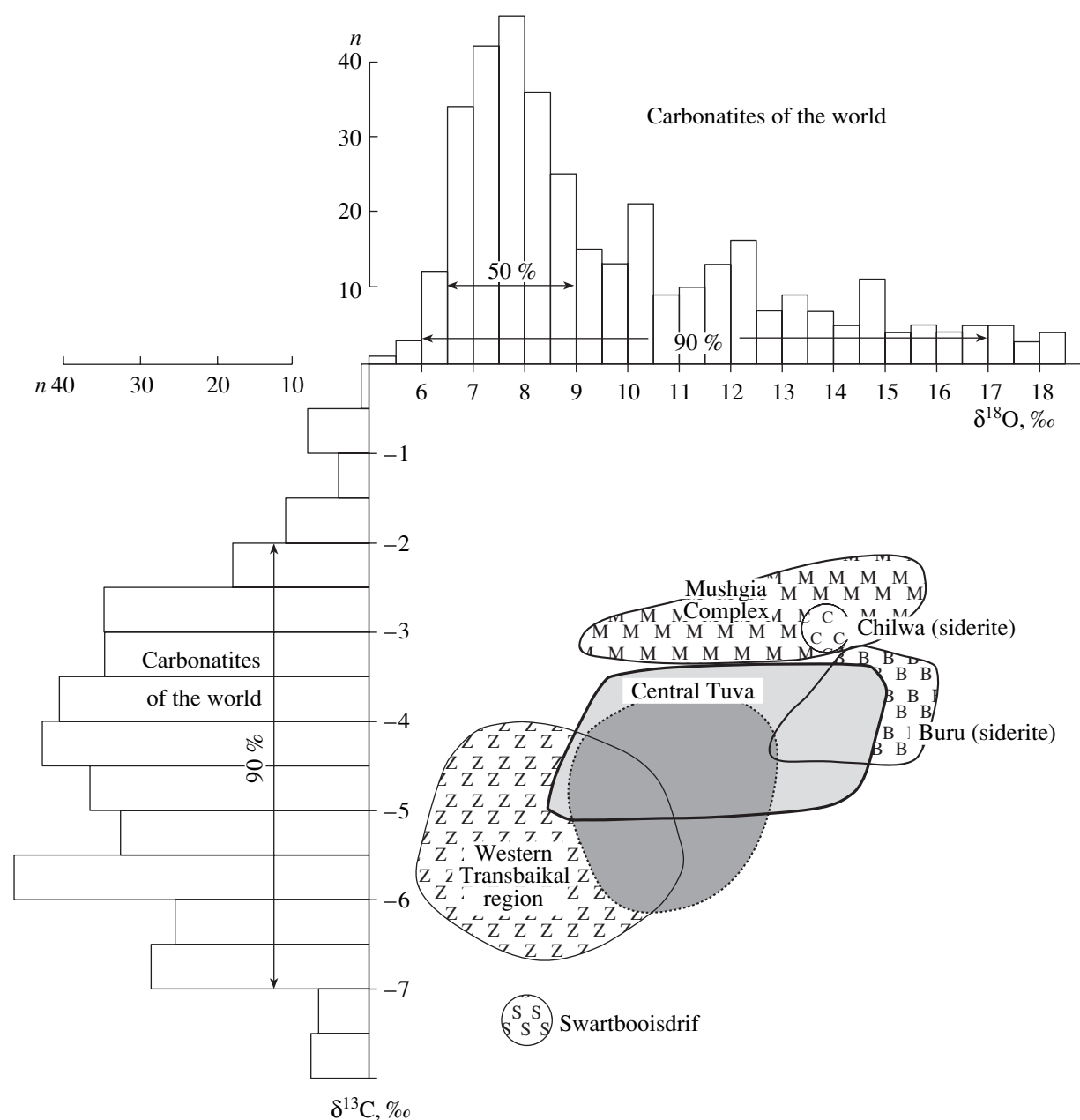


**Fig. 11.** Comparison of oxygen and carbon isotopic compositions of carbonatites from central Tuva and other provinces. Bar charts are data on intrusive carbonatites, after Deines (1989); isotopic compositions of carbonatites from the western Transbaikal region are given after Nikiforov et al. (2000); from the Mushgia Complex, Mongolia, after Kuleshov (1986); and of Chilwa, Buru, and Swartbooisdrif Fe-rich carbonatites, after Thompson et al. (2002).

tions of initial ratios ( $^{87}\text{Sr}/^{86}\text{Sr}$ )<sub>i</sub> in carbonatites and its obvious difference from the corresponding ratio in sedimentary rocks, which is estimated at 0.7062–0.7072 (Blokh and Dagaeva, 1987).

The primary O, C, S, and Sr isotopic compositions determined for carbonatites of central Tuva are consistent with those of carbonatites from other provinces.

The ranges of oxygen and carbon isotopic compositions of primary igneous carbonatites were estimated for the first time by Taylor et al. (1967) at  $\delta^{13}\text{C}$  varying

from  $-4$  to  $-8\text{‰}$  and  $\delta^{18}\text{O}$  varying from  $+6$  to  $+10\text{‰}$ . In the subsequent review by Deines (1989), it was shown that the C and O isotopic compositions of carbonatites are often beyond the above limits. About 90% of intrusive carbonatites have  $\delta^{13}\text{C}$  ranging from  $-2$  to  $-7\text{‰}$  and  $\delta^{18}\text{O}$  ranging from  $+6$  to  $+17\text{‰}$  (Fig. 11). A wide range of isotopic compositions of carbonatites is commonly regarded as a result of magma fractionation, degassing, and contamination and/or postmagmatic alteration in the process of interaction with hydrother-

mal, formational, and surface waters, as well as with atmospheric oxygen in the case of volcanic carbonatites.

In general, the oxygen and carbon isotopic compositions of primary carbonatites from central Tuva correspond to the worldwide estimates, differing from the latter by elevated  $\delta^{18}\text{O}$  values relative to the range from +6.5 to +9.0‰ (Fig. 11), which comprises about 50% of the oxygen isotopic compositions of carbonatites from other provinces (Deines, 1989). The aforementioned crustal contamination of melts may be regarded as a cause of enrichment in the heavy oxygen isotope. At the same time, this enrichment may be caused by specific features of the mantle source. It should be noted that the field of primary isotopic compositions of carbonatites was outlined largely from data obtained for alkaline ultrabasic complexes and differences in their compositions were explained by heterogeneity of mantle sources (Deines, 1989). Carbonatites from central Tuva are distinguished from classic carbonatites of alkaline ultrabasic complexes in many respects. First of all, no associated silicate rocks have been reliably established to date, and carbonatites themselves are depleted in silicate minerals. Furthermore, the studied carbonatites pertain to a rare group of ferrocarbonatites. The oxygen isotopic composition of these carbonatites determined by Bolonin and Zhukov (1983) and Thompson et al. (2002) is also characterized by high  $\delta^{18}\text{O}$  values (Fig. 11).

The enrichment of carbonatites from central Tuva in sulfur (both in sulfide and sulfate species) is another specific feature. Carbonatites from the Mountain Pass deposit (Mitchell and Krouse, 1971, 1975) are their analogues in this respect. The isotopic sulfur composition of minerals at that deposit is the same as that of carbonatites from central Tuva. Pyrite and barite are characterized by average  $\delta^{34}\text{S}$  equal to  $-4$  and  $+7$ ‰, respectively, and the difference between these values, as in siderite carbonatites at the Karasug deposit, is 12‰ on average.

A similar sulfur isotopic composition of barite and baritocelastine ( $\delta^{34}\text{S} = 3.4\text{--}13.0$ ‰) was determined for carbonatites from the western Transbaikal region, which are the closest analogues of the carbonatites under consideration (Nikiforov et al., 2000). Carbonatites of both regions are coeval (~120 Ma) and similar in geochemistry (high Sr, Ba, LREE, P, S, and F contents combined with depletion in Nb and Ta). They are characterized by similar O and C isotopic compositions; oxygen of carbonatites from the western Transbaikal region is also enriched in  $^{18}\text{O}$  ( $\delta^{18}\text{O} = 6.0\text{--}10.7$ ‰). The similarity in isotopic composition of carbonatites from central Tuva and the western Transbaikal region probably reflects a common geochemical specialization of their mantle sources, which differ from the sources of classic carbonatites related to alkaline ultrabasic complexes.

## CONCLUSIONS

(1) The performed isotopic study of minerals and whole-rock samples of ankerite–calcite and siderite carbonatites from central Tuva has shown that both carbonatite varieties are characterized by similar primary isotopic compositions:  $\delta^{18}\text{O}_{\text{carb}} = +(8.8\text{--}14.7)$ ‰,  $\delta^{13}\text{C}_{\text{carb}} = -(3.6\text{--}4.9)$ ‰,  $\delta^{18}\text{O}_{\text{quartz}} = +(11.6\text{--}13.7)$ ‰,  $\delta^{34}\text{S}_{\text{pyrite}} = +(0.3\text{--}1.1)$ ‰, and  $(^{87}\text{Sr}/^{86}\text{Sr})_i = 0.7042\text{--}0.7048$  for ankerite–calcite carbonatite and  $\delta^{18}\text{O}_{\text{sid}} = +(9.2\text{--}12.4)$ ‰,  $\delta^{13}\text{C}_{\text{sid}} = -(3.9\text{--}5.9)$ ‰,  $\delta^{18}\text{O}_{\text{quartz}} = +(11.2\text{--}11.4)$ ‰,  $\delta^{34}\text{S}_{\text{pyrite}} = -(4.4\text{--}1.8)$ ‰,  $\delta^{34}\text{S}_{\text{sulfate}} = +(8.6\text{--}14.5)$ ‰, and  $(^{87}\text{Sr}/^{86}\text{Sr})_i = 0.7042\text{--}0.7045$  for siderite carbonatite. The isotopic characteristics of both varieties allow us to suggest their common source comparable with that of the Late Mesozoic carbonatites in the western Transbaikal region and Mongolia.

(2) The age of both types of carbonatites was estimated at  $118 \pm 9$  Ma with the Rb–Sr method according to the isotopic composition of mica dispersed in these rocks.

(3) Carbonatite melts could have been contaminated to some extent with crustal materials enriched in radiogenic strontium and the heavy oxygen isotope. The contamination induced disequilibrium of isotopic compositions of rock-forming minerals in particular carbonatite samples and a relatively wide variation of their isotopic composition in the region as a whole.

(4) Isotopic compositions of carbonatites were markedly altered at the postmagmatic stage and under supergene conditions. The hydrothermal celestinization of some siderite carbonatite bodies in the Karasug field was accompanied by a gain of radiogenic strontium. The supergene alteration resulted in modification of the O, C, and Sr isotopic compositions. Carbonates were appreciably enriched in  $^{18}\text{O}$  and  $^{87}\text{Sr}$ . Variations of carbon isotopic composition did not have a systematic character.

## ACKNOWLEDGMENTS

We thank Yu.A. Kostitsyn for his critical comments, which allowed us to improve the paper.

This study was supported by the Russian Foundation for Basic Research (project nos. 03-05-64585, 06-05-64235, and 06-05-64841) and by the Council for Grants of the President of the Russian Federation for Support of Leading Scientific Schools (grant no. NSh-1145.2003.5).

## REFERENCES

1. A. M. Blokh and I. V. Dagaeva, "Origin of Sulfates from Middle Paleozoic Sedimentary Sequences in the Tuva Trough," *Sov. Geol.*, No. 10, 91–99 (1987).
2. A. V. Bolonin and A. V. Nikiforov, "Chemical Composition of Minerals from Carbonatites of the Karasug Deposit in Tuva," *Geol. Rudn. Mestorozhd.* **46** (5), 427–443 (2004) [*Geol. Ore Deposits* **46** (5), 372–386 (2004)].



3. A. V. Bolonin and F. I. Zhukov, "C, O, and S Isotopic Characteristics of Carbonatites from a Mineral Deposit in Southern Siberia," *Izv. Vyssh. Uchebn. Zaved., Geol. Razved.*, No. 9, 67–72 (1983).
4. A. V. Bolonin, T. M. Kaikova, and G. M. Komarnitsky, "The Carbonatite Origin of an Iron–Fluorite–Barite–Rare Earth Element Deposit," *Izv. Vyssh. Uchebn. Zaved., Geol. Razved.*, No. 3, 59–64 (1984).
5. I. V. Chernyshev, N. I. Serdyuk, D. Z. Zhuravlev, et al., "High-Precision Strontium Isotopic Analysis Using One-Filament Ionization Mode," in *Mass Spectrometry and Isotopic Geology* (Nauka, Moscow, 1983), pp. 30–43 [in Russian].
6. P. Deines, "Stable Isotope Variation in Carbonatites," in *Carbonatites: Genesis and Evolution* (Unwin Hyman, London, 1989), pp. 301–359.
7. *Geological Map of the Tuvinskaya ASSR, Scale 1 : 500000*, Ed. by A. A. Podkamenny and M. L. Sherman (VSEGEI, Leningrad, 1983) [in Russian].
8. R. L. Hay and J. R. O'Neil, "Carbonatite Tuffs in the Laetolil Beds of Tanzania and the Kaiserstuhl in Germany," *Contrib. Mineral. Petrol.* **82**, 403–406 (1983).
9. M. N. Kandinov and E. S. Kharlamov, "Physicochemical Conditions of Fluorite Formation from Halogenic–Alkaline Melt-Brines," in *Theory and Practice of Thermobarogeochemistry* (Nauka, Moscow, 1978), pp. 137–138 [in Russian].
10. A. P. Khomyakov and E. I. Semenov, *Hydrothermal Deposits of Rare Earth Fluorocarbonates* (Nauka, Moscow, 1971) [in Russian].
11. V. N. Kuleshov, *Isotopic Characteristics and Origin of Deep Carbonatites* (Nauka, Moscow, 1986) [in Russian].
12. N. A. Kulik and S. V. Mel'gunov, "Evolution of Mineralization in Multicomponent Hematite–Fluorite–Bastnaesite Occurrences of Southern Tuva," *Geol. Geofiz.* **33** (2), 93–103 (1992).
13. K. R. Ludwig, *ISOPLOT/Ex. Version 2.49. A Geochronological Toolkit for Microsoft Excel* (Berkeley Geochronology Center Spec. Publ., 2001), No. 1a.
14. R. H. Mitchell and H. R. Krouse, "Isotopic Composition of Sulfur in Carbonatite at Mountain Pass, California," *Nature* **231**, 182 (1971).
15. R. H. Mitchell and H. R. Krouse, "Sulphur Isotope Geochemistry of Carbonatites," *Geochim. Cosmochim. Acta* **39**, 1505–1513 (1975).
16. A. V. Nikiforov, A. V. Bolonin, A. M. Sugorakova, et al., "Carbonatites of Central Tuva: Geological Structure, Mineral and Chemical Composition," *Geol. Rudn. Mestorozhd.* **47** (4), 1–23 (2005) [*Geol. Ore Deposits* **47** (4), 326–345 (2005)].
17. A. V. Nikiforov, V. V. Yarmolyuk, B. G. Pokrovsky, et al., "Late Mesozoic Carbonatites of Western Transbaikalia: Mineralogical, Chemical, and Isotopic (O, C, S, Sr) Characteristics and Relationships to Alkaline Magmatism," *Petrologiya* **8** (3), 309–336 (2000) [*Petrology* **8** (3), 278–283 (2000)].
18. H. Ohmoto and R. O. Rye, "Isotopes of Sulfur and Carbon," in *Geochemistry of Hydrothermal Ore Deposits* (Wiley, New York, 1979), pp. 509–567.
19. D. O. Ontoev, "Problems of Geology of Fluorine–Rare Earth–Iron Deposits," *Geol. Rudn. Mestorozhd.* **5** (6), 18–33 (1963).
20. B. G. Pokrovsky, *Crustal Contamination of Mantle Magmas from Isotope Geochemistry Data* (Nauka, Moscow, 2000) [in Russian].
21. L. S. Puzanov, "Genetic Type of Fluorite–Barite–Iron Mineralization in the Tuvinskaya ASSR," *Dokl. Akad. Nauk SSSR* **225** (3), 669–672 (1975).
22. H. Sakai, T. J. Casadevall, and J. G. Moore, "Chemistry and Isotope Ratios of Sulfur in Basalts and Volcanic Gases at Kilauea Volcano, Hawaii," *Geochim. Cosmochim. Acta* **46**, 729–738 (1982).
23. H. Sakai, D. J. Des Marais, A. Ueda, and J. C. Moore, "Concentrations and Isotope Ratios of Carbon, Nitrogen, and Sulphur in Ocean-Floor Basalts," *Geochim. Cosmochim. Acta* **48**, 2433–2441 (1984).
24. L. D. Shorygina, *Cenozoic Stratigraphy of Western Tuva* (Tr. Geol. Inst. Akad. Nauk SSSR, Moscow, 1960), Vol. 26, pp. 165–203.
25. V. V. Shurupov, N. I. Plevaya, and S. L. Mirkina, "Mesozoic Mineralization and Hydrothermal Alteration of Some Intrusive Rocks in Tuva," in *Absolute Dating of Tectonomagmatic Cycles and Stages of Ore Mineralization from 1964 Data* (Nauka, Moscow, 1966), pp. 317–325 [in Russian].
26. B. E. Taylor, "Magmatic Volatiles: Isotopic Variations of C, H, and S," *Reviews in Mineral.* **16**, 185–225 (1986).
27. H. P. Taylor, J. Frechen Jr., and E. T. Degens, "Oxygen and Carbon Isotope Studies of Carbonatites from the Laacher See District, West Germany and the Alno District, Sweden," *Geochim. Cosmochim. Acta* **31**, 407–430 (1967).
28. R. N. Thompson, P. M. Smith, S. A. Gibson, et al., "Ankerite Carbonatite from Swartbooisdrif, Namibia: the First Evidence for Magmatic Ferrocyanatite," *Contrib. Mineral. Petrol.* **143**, 377–395 (2002).
29. Y. F. Zheng, "Oxygen Isotope Fractionation in Carbonate and Sulfate Minerals," *Geochem. J.* **33**, 109–126 (1999).
30. Y. F. Zheng and K. Simon, "Oxygen Isotope Fractionation in Hematite and Magnetite: A Theoretical Calculation and Application to Geothermometry of Metamorphic Iron-Formation," *Eur. J. Mineral.* **3**, 877–886 (1991).
31. D. Z. Zhuravlev, I. V. Chernyshov, A. A. Agapova, and N. I. Serdyuk, "High-Precision Neodymium Isotopic Analysis of Rocks," *Izv. Akad. Nauk SSSR, Ser. Geol.*, No. 12, 23–40 (1983).